Aptamers functionalized metal and metal oxide nanoparticles: Recent advances in heavy metal monitoring

Simona Sawan, Abdelhamid Errachid, Rita Maalouf, Nicole Jaffrezic-Renault

Aptamers functionalized metal and metal oxide nanoparticles: Recent advances in heavy metal monitoring

Simona Sawan[1,2], Abdelhamid Errachid[1], Rita Maalouf[2*], Nicole Jaffrezic-Renault[1*]

[1]Institut des Sciences Analytiques, Université de Lyon, Claude Bernard Lyon 1, UMR 5280, CNRS - 5, rue de la Doua, 69100 Villeurbanne, France.

[2]Department of Sciences, Faculty of Natural and Applied Sciences, Notre Dame University - Louaize, Zouk Mosbeh, Lebanon.

Abstract

Heavy metal contamination has long been a major hazard to the entire ecological system and human beings. Consequently, sensitive and reliable methods have been developed for the detection of heavy metal ions from different systems. Advancements in biotechnology, and in functional nucleic acids specifically, have offered new methods for heavy metal monitoring based on the specific interactions of aptamers with heavy metal ions. The introduction of nanoparticles to aptamer-based technologies has also presented its advantages of increased immobilization efficiency, sensitivity and selectivity. Thus, this review provides an update on the progress of using aptamers functionalized nanoparticles for the monitoring of heavy metal ions. The aptamer-based detection of heavy metal ions using metallic and metallic oxide nanoparticles are emphasized. Even though gold nanoparticles are the most commonly used with aptamers for the detection of heavy metal ions reporting extremely low detection limits, several other nanoparticles have emerged as promising modifications to aptamers in heavy metal monitoring as well. Comparing the different techniques used, electrochemical methods have presented the best performance while offering their advantages over optical and spectrometric techniques.

Keywords

Heavy metals, metal nanoparticles, metal oxide nanoparticles, aptamers, oligonucleotides, detection, adsorption

1. Introduction

The upsurge in waste materials whether agricultural, industrial or medical has resulted in an increased risk of the population's exposure to pollutants including organic molecules and heavy metals [1]. Heavy metals are neither biodegradable nor environmentally degradable, tending to accumulate in living beings through the food chain [2]. Consequences of heavy metal exposure include diseases and disorders in several systems, and their severity depends on the heavy metal, way of exposure and concentration. The side effects of heavy metals on human beings and the environment have led several organizations including the World Health Organization (WHO) to set safety limits. However, reaching these limits in some parts of the world can be somehow challenging due to rapid urbanization and industrialization [3]. Thus, speciation analysis and quantitative determination of toxic metals are of great importance.

Several methods have been employed for the detection of toxic heavy metals from different matrices. These include inductively coupled plasma mass spectrometry ICP-MS [4], inductively coupled plasma optical emission spectroscopy ICP-OES [5], inductively coupled plasma atomic emission spectroscopy ICP-AES [6], atomic absorption spectroscopy AAS [7] and cold vapor atomic fluorescence spectroscopy CV-AFS [8]. Despite the advantages of low limits of detection and high sensitivities offered by these techniques, some challenges still exist. These techniques are expensive, with a complex operational procedure, long detection time and difficulty of on-site monitoring [9].

Aptamers are typically artificial oligonucleotides (mainly single-stranded DNA or RNA) or peptides produced by systematic evolution of ligands by exponential enrichment (SELEX) method in vitro. They present one type of functional nucleic acids that can form binding pockets and clefts within a well-defined three-dimensional structure for the specific recognition of target molecules [10] such as metal ions, peptides and proteins, cells. They offer the advantages of specificity, easy and cost-effective preparation and modification and high binding affinity compared to small-molecule ligands [11]. They are known for their high temperature and chemical stability, as well as their target versatility. Accordingly, several bio-sorbents and biosensors have been designed based on these specific interactions. Additionally, aptamers designed for heavy metal sensors can be easily regenerated, and the sensors can be reused.

In recent years, nanotechnology has emerged as an interdisciplinary technology with numerous fields including physics, biology, chemistry, medicine and material science due to the predefined superstructure of nanoparticles [9]. Nanomaterials can be easily functionalized with different substrates through covalent bonding or non-covalent actions.

Combining aptamers and nanoparticles in sensors have presented several advantages over using conventional methods. Not only do they exhibit dual properties pertaining to each element alone, but they also demonstrate new properties that can be useful in many applications. Utilizing nanomaterials with aptamers can convert the interaction between aptamers and their substrates into electrical, optical and other signals. The use of nanoparticles increases the surface area of the used material thus increasing the density of the immobilized aptamers and the area of interaction between these aptamers and analyte molecules [12].

Several reviews have been published recently focusing on biosensors for specific heavy metals such as mercury [13], lead [14] and arsenic [15]. Other reviews have focused on techniques

such as electrochemical techniques [16] or optical techniques [17]. In this review, an updated overview of the aptamer-based approaches developed in the past five years for the analysis of heavy metals by using metal and metal oxide nanoparticles is presented.

2. Interaction between heavy metals and nucleic acids

Metal ion coordination to single stranded nucleic acids has been reviewed, taking into consideration the phosphate diester backbone [18]. It was reported that metal ions can bind to the phosphate backbone stabilizing the DNA duplex. Nevertheless, such interaction disregards the chemical nature of the metal ions and DNA. The ability of cations to bind nucleobases can be ascribed to the cation's ionic radius, coordination behavior and hydration effects. Sigel and Sigel summarized the nucleotide coordination affinity to various divalent ions [19]. It was shown that each nucleobase has a preferred binding site for the different metals.

The different and specific interactions between the nucleobases of aptamers and single-stranded DNA from one side, and heavy metal ions from the other side, have been the basis of heavy metal detection by DNA. Most commonly, mercury Hg^{2+} and silver Ag^{+} ions recognition has been based on thymine (T)-thymine and cytosine (C)-cytosine mismatches to form the more stable T-Hg^{2+}-T and C-Ag^{+}-C complexes [20, 21]. Pb^{2+} ions have been detected using the conformational switch of a guanine (G)-rich aptamer from random coil to G-quadruplex structure [22], whereas cadmium Cd^{2+} ions were captured using thymine and guanine-rich aptamers [11]. The detection mechanism differs depending on how the nucleobases make up the aptamer. The aptamer functionalization of nanoparticles can be either through adsorption or chemical bonding also leading to different sensing mechanisms.

3. Metal nanoparticles

In addition to the increased surface area due to their small sizes, metallic nanoparticles present several advantages including an increased sensitivity [12]. The various metallic nanoparticles that have been combined with aptamers for the detection of heavy metals are detailed in this section.

3.1. Gold nanoparticles

Aptamer-based strategies using gold nanoparticles (Au NPs) are the most common for the study of heavy metals. Au NPs are known for their easy and controllable synthesis as well as stability [23]. For the detection of heavy metals, gold nanoparticles have been integrated with aptamers either as a deposited layer on the surface of the signal transducer, or as a conjugated form with the aptamer.

Electrochemical approaches are the most common aptamer-based strategies using gold nanoparticles, among which, differential pulse voltammetry (DPV) is the most used. Other electrochemical techniques include square wave voltammetry (SWV), electrochemical impedance spectroscopy (EIS), differential pulse stripping voltammetry (DPSV), differential pulse anodic stripping voltammetry (DPASV), electrochemiluminescence (ECL), photoelectrochemistry (PEC) chronocoulometry, and amperometry. The most recent applications are summarized in Table 1. Using electrochemistry, mercury is the most frequently studied heavy metal, making use of the thymine – mercury – thymine interaction. Other heavy metal ions detected include lead, cadmium, arsenic and silver. It is worth noting that several authors have used gold nanoparticles in combination with other metal and metal oxide nanoparticles such as silver nanoparticles Ag NPs [1, 24] and iron oxide nanoparticles Fe_3O_4 NPs [3, 25].

Table 1 Electrochemical aptasensors using gold nanoparticles for the detection of heavy metals

From Table 1, it can be noticed that amongst the different studies, lead, mercury and arsenic were the major investigated metals. Almost all aptamers utilized for mercury detection are thymine-rich, and electrochemiluminescence along with differential pulse voltammetry are the two most used techniques. The lowest limit of detection (2 aM) was reported using electrochemiluminescence with two DNA strands; one immobilized on Fe_3O_4@SiO_2/dendrimers/QD and the other with gold nanoparticles. As shown in figure 1a, the nanoparticles/DNA probe was dropped and adsorbed on an indium tin oxide electrode using a magnetic field exhibiting an amplified ECL signal. A second probe made up of gold nanoparticles and another aptamer was hybridized with the first strand resulting in the quenching of the signal. To measure the signal corresponding to different heavy metal concentrations, the electrode was incubated with Hg^{2+} and as a result, the second probe was separated from the electrode leading to a change in the ECL signal [25]. The authors attributed this low LOD to several factors including the high electron transfer rate of the modifiers used, high spectral overlap of QDs and Au NPs and the specific interaction between thymine and Hg^{2+}. As promising as this sensor seems, some points such as the complex preparation and reusability need to be addressed. Interestingly, most of the lowest LODs for Hg^{2+} detection were reported using electrochemiluminescence [25-29].

In the case of the detection of lead, all the aptamers used were guanine-rich aptamers, with differential pulse voltammetry as the most used electrochemical technique. However, except for one study, the lowest LODs (as low as 4×10^{-5} nM) were obtained when no modifiers were added to the gold nanoparticles and aptamers [12, 22, 30-32]. In one of the studies with the lowest LOD and widest linear range [30], an aptasensor was developed based on electrochemiluminescence resonance energy transfer. Au NPs were used to modify an electrode followed by the addition of carbon nitride nanofibers and $Ru(phen)_3^{2+}$ and hybridized complementary aptamers. In absence of

Pb^{2+}, $Ru(phen)_3^{2+}$ can be captured on the electrode through the grooves of the aptamers thus leading to an ECL signal. In presence of Pb^{2+}, $Ru(phen)_3^{2+}$ would be detached thus inhibiting the signal (figure 1b). For arsenic (As(III)), the best analytical performance was obtained by Ensafi et al. [33]. The proposed mechanism involved the modification of a glassy carbon electrode with reduced graphene oxide, gold nanoparticles and a thiolated aptamer. Electrochemical impedance spectroscopy increased after incubation in arsenic solution leading to its detection with an LOD of 1.4×10^{-7} ng.mL^{-1} (figure 1c).

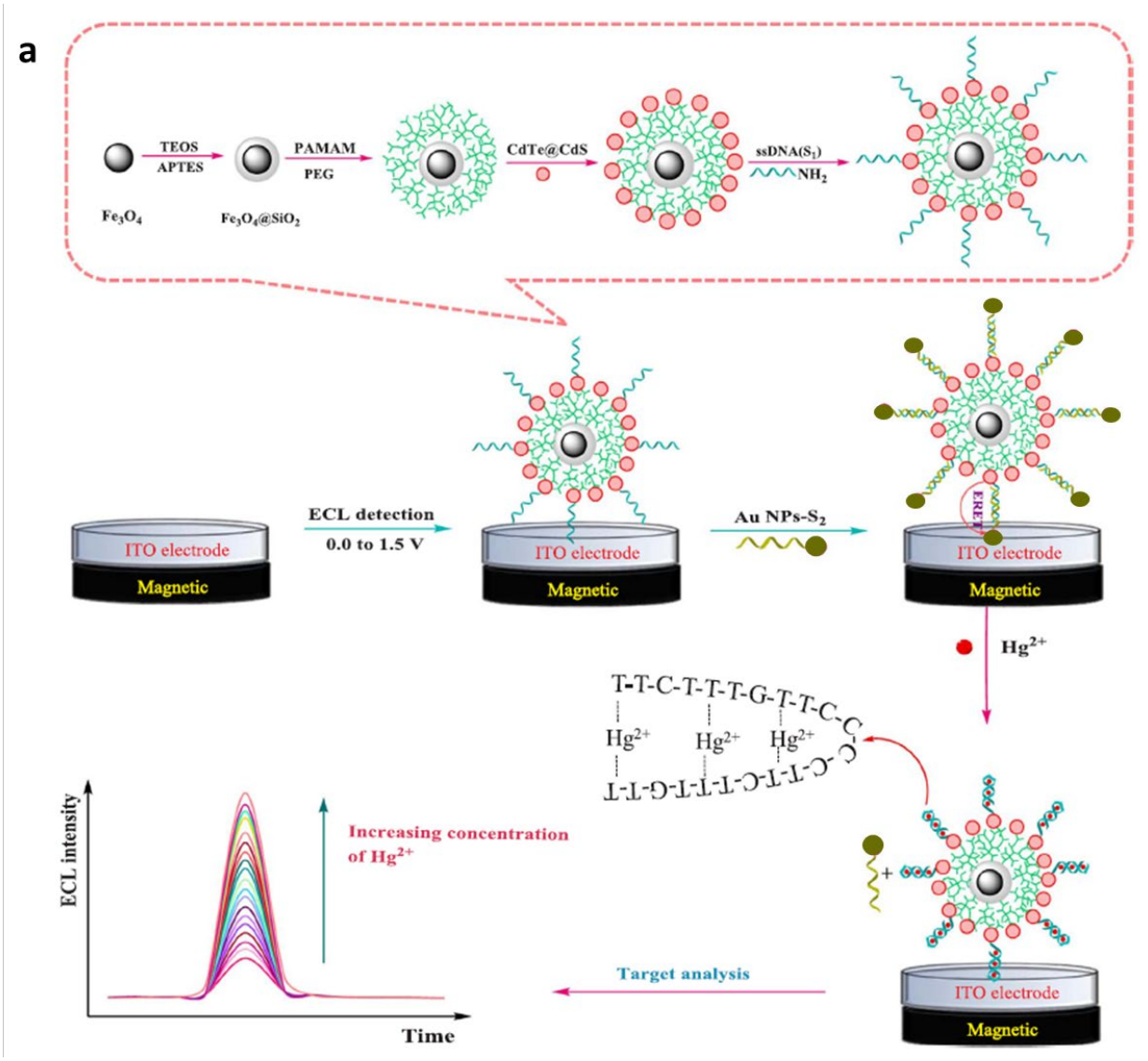

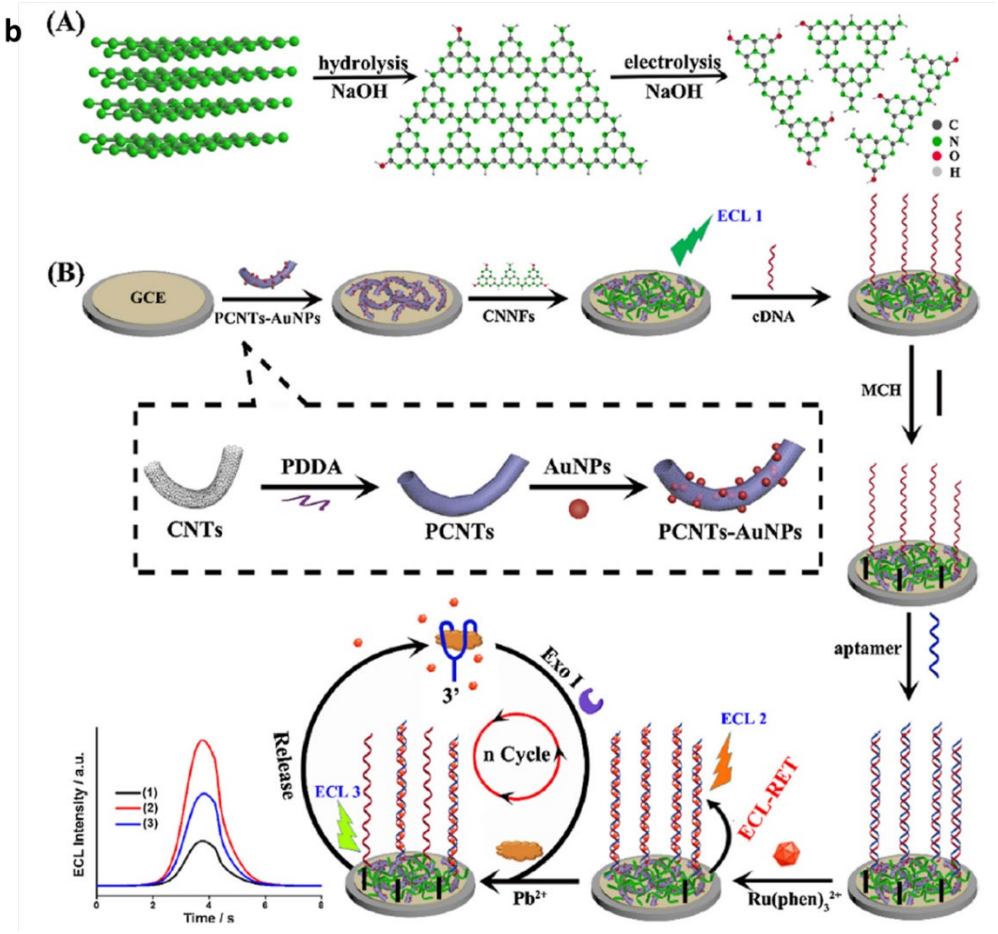
b
(A)
hydrolysis
NaOH
electrolysis
NaOH
C
N
O
H
(B)
GCE
PCNTs-AuNPs
CNNFs
ECL 1
cDNA
MCH
CNTs
PDDA
PCNTs
AuNPs
PCNTs-AuNPs
aptamer
3'
Exo I
n Cycle
Release
ECL 2
ECL 3
ECL-RET
ECL Intensity / a.u.
(1)
(2)
(3)
Time / s
Pb2+
Ru(phen)3 2+

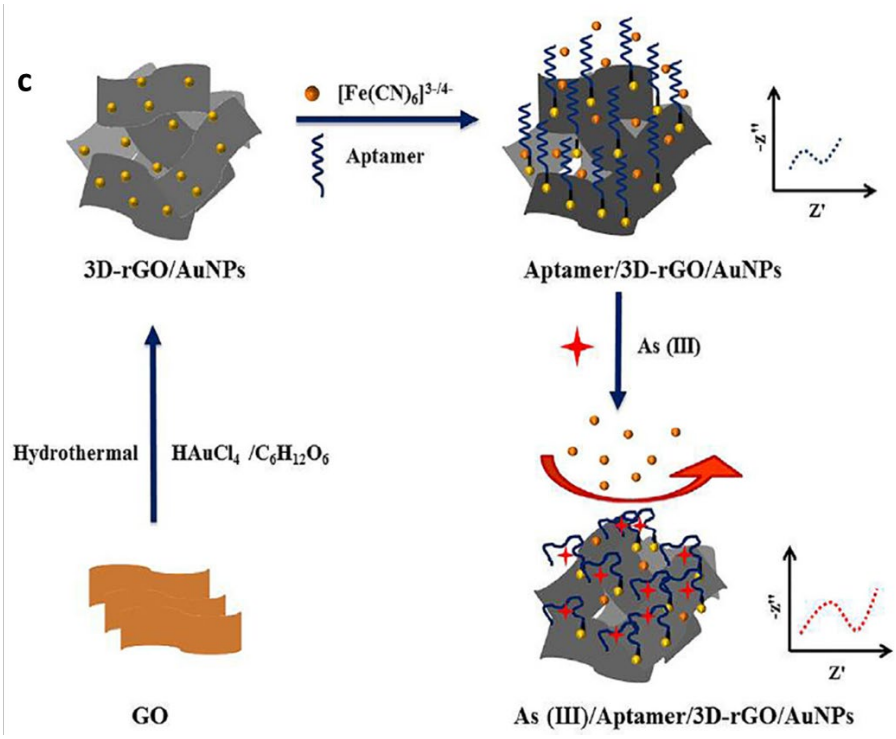
c
[Fe(CN)6]3-/4-
Aptamer
-Z''
Z'
3D-rGO/AuNPs
Aptamer/3D-rGO/AuNPs
As (III)
Hydrothermal
HAuCl4 /C6H12O6
GO
As (III)/Aptamer/3D-rGO/AuNPs

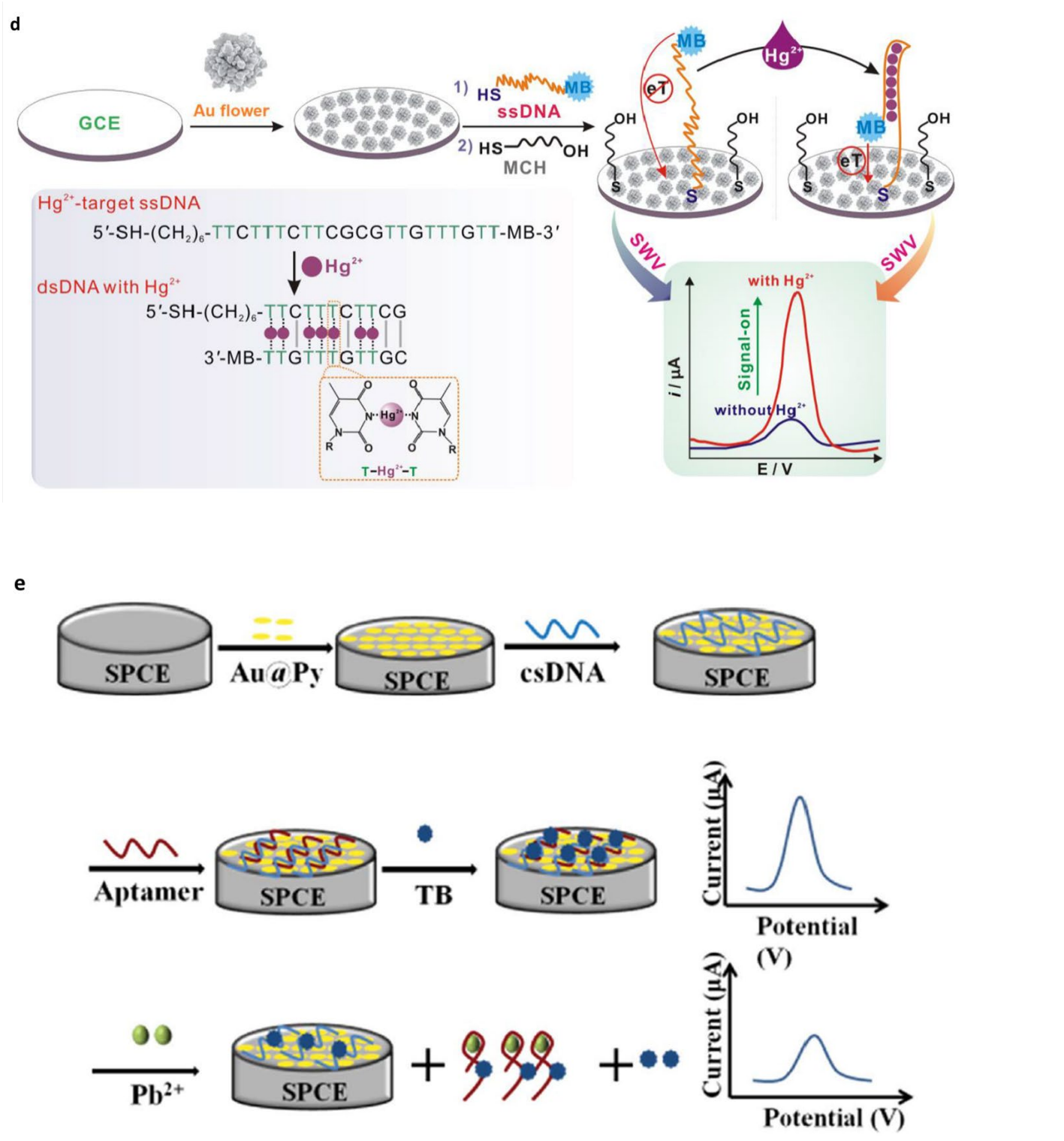

Figure 1: (a) Schematic representation of the ECL biosensor for Hg^{2+} detection [25]. Reproduced with permission from Elsevier, (b) Schematic illustration of (A) two-step strategy for preparation

of carbon nitride nanofibers CNNFs and (B) fabrication of the proposed aptasensor for Pb^{2+} detection [30]. Reproduced with permission from Elsevier, (c) The mechanism reaction of the proposed aptasensor based on 3D-reduced graphene oxide modified gold nanoparticles for determination of arsenite [33]. Reproduced with permission from Elsevier. (d) Illustration of the single-step and specific detection of Hg^{2+} by using Au flowers-based electrochemical aptasensor. Lower left: conformational change of single-stranded DNA (ssDNA) upon binding to Hg^{2+}. Reprinted (adapted) with permission from [34]. Copyright 2018 American Chemical Society, (e) Presentation of the Pb^{2+} biosensor and detection principle. Reproduced from Ref. [35] with permission from the Royal Society of Chemistry

In general, the sensing mechanisms differed between the reported studies. Sensor designs using the combination of gold nanoparticles and aptamers for the detection of various analytes are numerous; however, for the detection of heavy metals, a few immobilization techniques and sensing mechanisms are common. The sensing mechanism depends on how the nanoparticles and aptamers are fixed on the electrode, and on the detection method used. Most mechanisms relied on using gold nanoparticles as an immobilization layer for the aptamers. When one aptamer was immobilized on the nanoparticles, the detected signals were mainly the result of the formation or disassembly of stable structures such as G-quadruplex and hairpin. For example, Zhang et al. proposed a sensor for Hg^{2+} using methylene blue-tagged aptamers and gold nanoparticles. In presence of mercury ions, the aptamer formed a hairpin structure and a limit of detection of 0.62 fM was obtained (figure 1d) [34]. In other cases, when two aptamers were used, the signal was due to the formation of a double helix, or its disassembly to form a more stable structure. A few studies have utilized gold nanoparticles as signal amplifiers and not for aptamer immobilization.

Ding et al. prepared an Au@Py modified screen-printed electrode with an aptamer and a complementary strand for the detection of $Pb^{2+}$to obtain an LOD of 0.6 ppb [35] (figure 1e).

Several other approaches than electrochemistry have combined gold nanoparticles with aptamers for the detection of heavy metal ions (Table 2). The heavy metal ion that was widely investigated using the different techniques is mercury. Colorimetry has been extensively utilized for the detection of lead, mercury, arsenic, cadmium and platinum. In most cases, Au NPs were used alone; however, a few studies have reported the use of magnetic nanoparticles among other modifications. Several detection strategies were employed. Unlike with electrochemical techniques, gold nanoparticles were mainly utilized as signal amplifiers making use of their catalytic and electrical properties. A lot of studies also relied on the change in color between colloidal gold nanoparticles (red) and aggregated nanoparticles (blue). Despite the expansive development of the detection mechanisms, the lowest limit of detection reported was 1.4 pM for the detection of mercury [36]. In this study, gold nanoparticles followed by the first aptamer were immobilized on a glass slide. The slide was put in contact with a solution containing mercury ions and the second aptamer which led to the adsorption of Hg^{2+} on AuNPs because of the hybridization of the two aptamers. This was followed by washing with Au NPs and observation under dark field microscopy (figure 2a). Comparing the studies involving cadmium ions, the lowest limit of detection was reported by Xu et al. [37]. The reported method used an aptamer competitive binding assay. The aptamer and PDDA were first combined by electrostatic interaction and the Au NPs were left free in the solution giving it its wine-red color. Upon the addition of the target ion, some aptamers could bind to it while others remain bound to PDDA leading to the aggregation between excess PDDA and Au NPs and changing the color of the solution with sufficient amounts of Cd^{2+} to blue. The signal could even be reported using a smartphone (figure 2b).

Only a few studies aimed at detecting arsenic ions colorimetrically in the past five years. Two of those studies [38, 39] use the same aptamer named Ars-3 that was reported in 2009 with a high affinity to both As (III) and As (V). Ever since, over 20 papers have aimed to detect As (III) using this aptamer. However, after Zong and Liu investigated the selective binding of arsenic to this aptamer [40], they showed that As (III) inhibited DNA adsorption without a significant effect on the stability of gold nanoparticles. In fact, upon comparing Ars-3 with a random sequenced DNA, similar color changes were observed. Thus, it was deduced that this method doesn't reflect aptamer binding to Arsenic, but rather adsorption of the analyte. As a result, the number of papers reporting the use of Ars-3 for As (III) detection decreased significantly, and other aptamers were studied [41].

Hu et al. investigated the interaction of Hg (II) and AuNPs and the role of Hg (II) on DNA adsorption to AuNPs. Upon increasing the concentration of mercury ions, opposite colorimetric trends were observed based on unwashed and washed AuNPs. Several DNA sequences were examined and found unimportant for the experimental outcome, suggesting that for this Hg (II) sensing strategy, Hg (II) adsorption to AuNPs needs to be considered [42].

A number of studies have used fluorometry for the detection of lead [23, 43, 44] and mercury [45, 46]. Most of the mechanisms that use fluorescence assume that the detection is based on the fluorescence quenching property of nanoparticles upon aptamer adsorption. Desorption of the aptamer due to its binding to target molecules results in fluorescence enhancement. Interestingly, the LODs were in the nanomolar range. Surface enhanced Raman spectroscopy (SERS) was also used for the detection of lead, mercury and arsenic [47-49]. The lowest limit of detection (0.4 pM) using a non-electrochemical technique was obtained using this method [49]. In this study, an aptamer was immobilized on gold nanoparticles through thiols and the resultant

aptamer embedded AuNPs were encapsulated with silver and hybridized with a complementary aptamer. In the absence of Hg^{2+}, a SERS signal was detected; however, in presence of Hg^{2+}, the first aptamer changes into a hairpin structure due to the interaction between the heavy metal ion and thymine separating the duplex and changing the SERS signal (figure 2c).

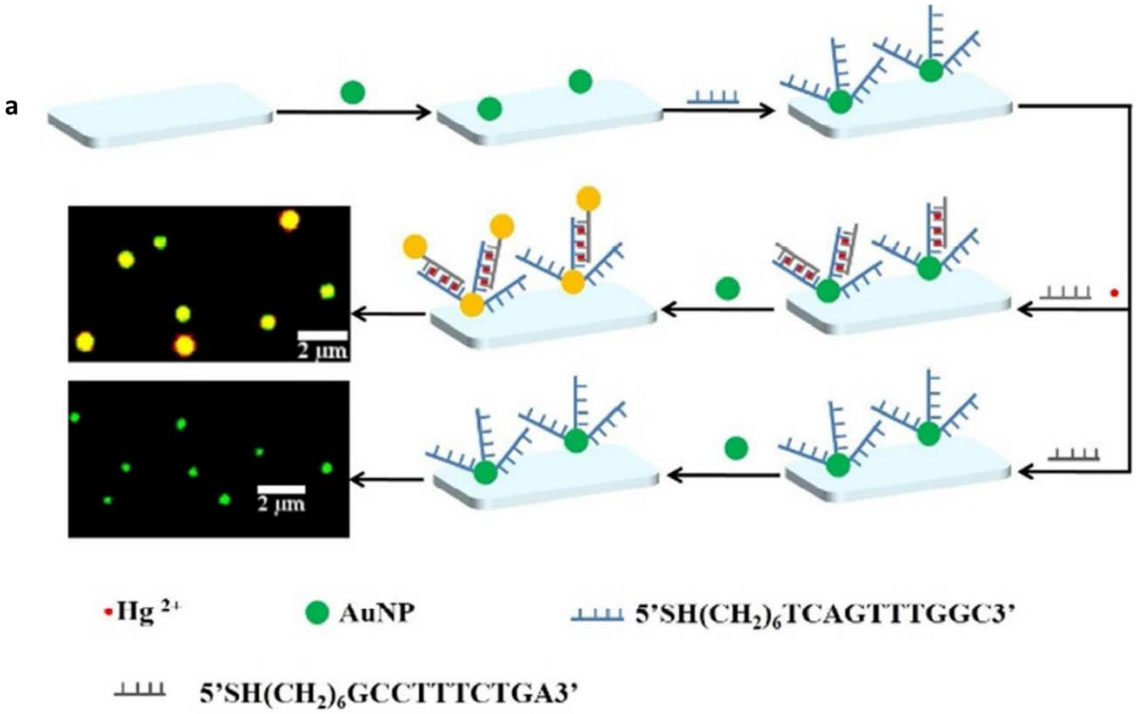

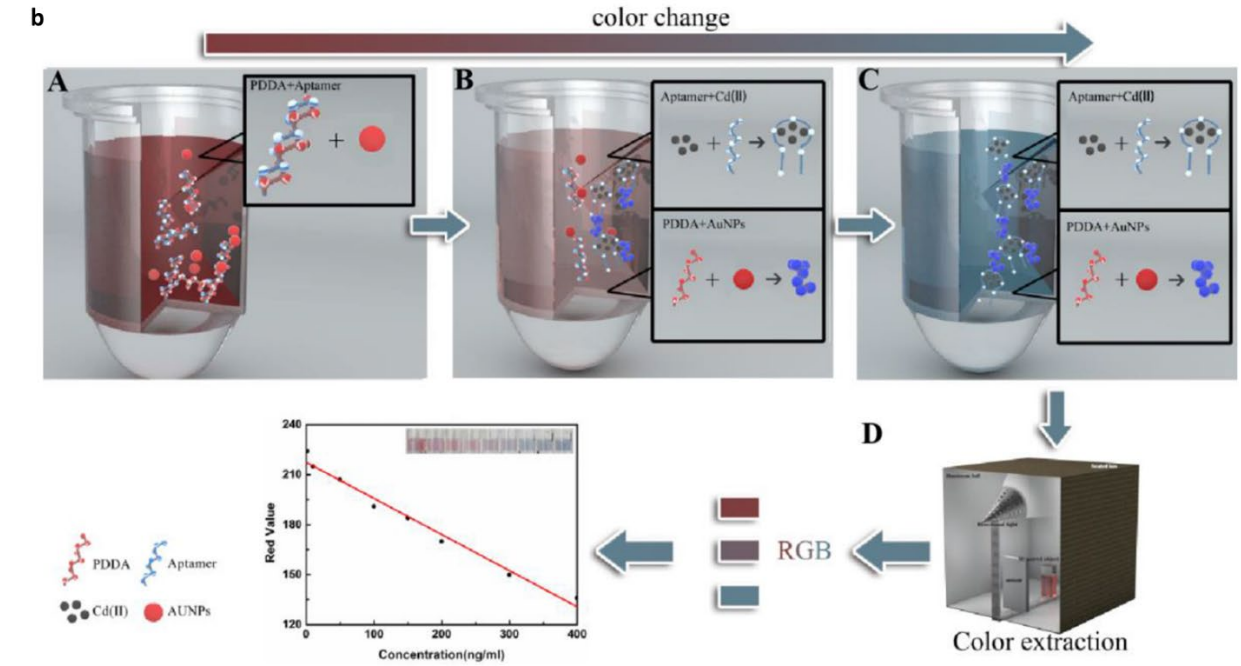
b
color change
A
PDDA+Aptamer
B
Aptamer+Cd(II)
PDDA+AuNPs
C
Aptamer+Cd(II)
PDDA+AuNPs
D
Color extraction
RGB
Red Value
Concentration(ng/ml)
PDDA
Aptamer
Cd(II)
AUNPs

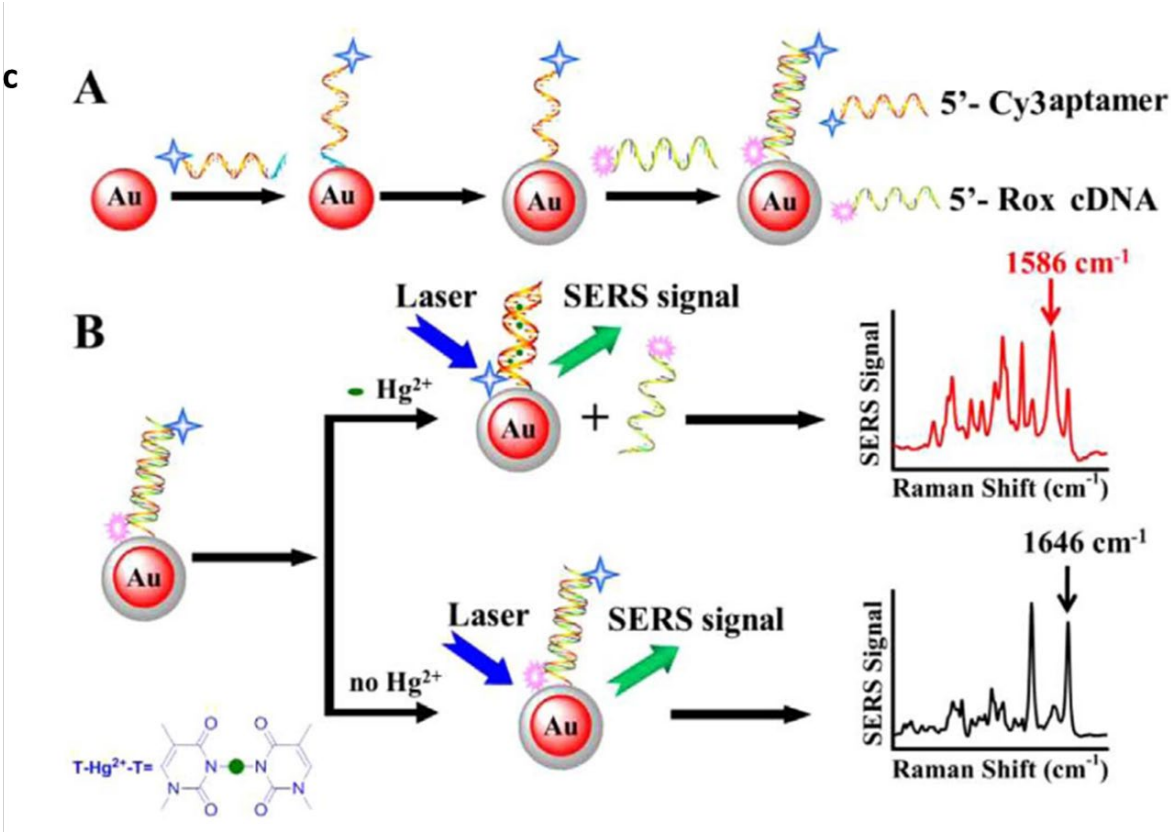
c
A
5'- Cy3aptamer
5'- Rox cDNA
Au
B
Laser
SERS signal
Hg2+
no Hg2+
1586 cm-1
1646 cm-1
SERS Signal
Raman Shift (cm-1)
T-Hg2+-T=

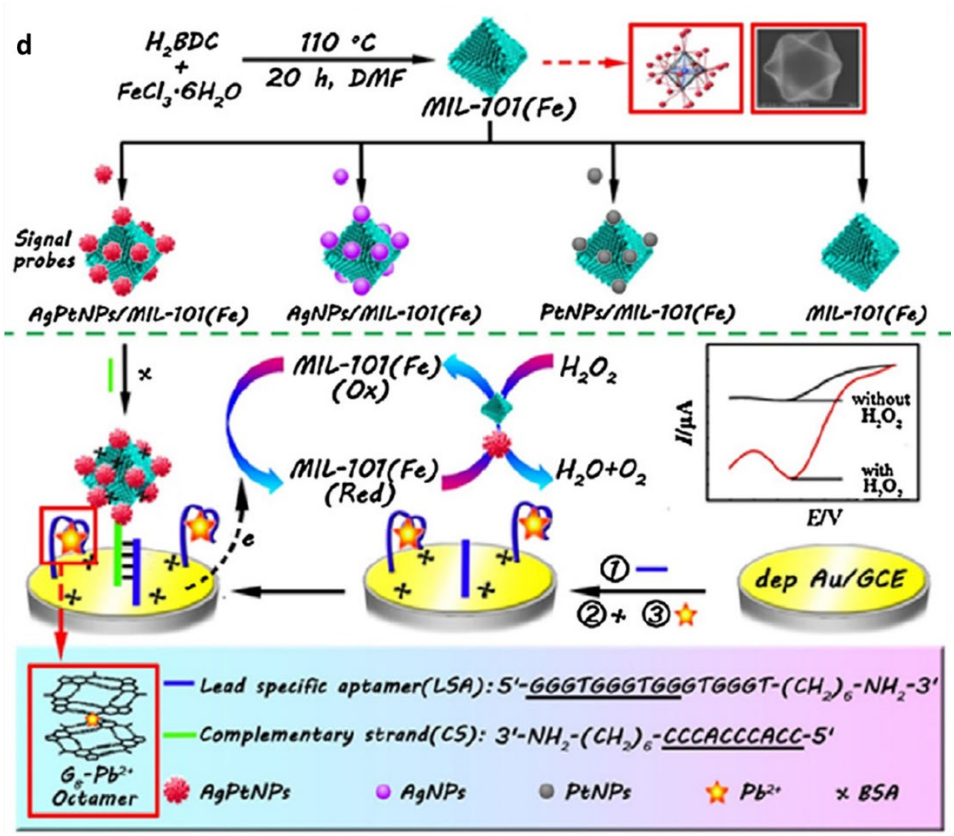

Figure 2: (a) Scheme of Hg^{2+} sensor at single-particle level with dark-field microscopy. Reprinted (adapted) with permission from [36]. Copyright 2018 American Chemical Society, (b) Schematic illustration of the colorimetric method. (A) Gold nanoparticles (AuNPs) incubated with aptamer and polydiene dimethyl ammonium chloride (PDDA); the color of the free AuNP solution was wine red; (B) AuNPs incubated with the aptamer, PDDA, and few Cd(II); the color of partial aggregation of the AuNP solution changed to reddish; (C) AuNPs incubated with the aptamer, PDDA, and sufficient Cd(II); the color of aggregation of the AuNP solution changed to blue; and (D) The red(R) values of the solution recorded with a smart phone [37], (c) (A) Fabrication of the dsDNA-embedded Au@Ag core-shell NPs. (B) The principle of ratiometric SERS aptasensor for Hg^{2+} detection [49]. Reproduced with permission from Elsevier. (d) Schematic illustration of the fabrication process of the proposed Pb2+ electrochemical aptasensor, together with the preparation

of different signal probes, and the mechanism of the signal amplification in the electrode interface [50]. Reproduced with permission from Elsevier.

In 2019, Zhang et al. studied the adsorption and desorption of DNA from gold nanoparticles and graphene oxide using fluorescence and concluded that DNA cannot be desorbed easily from gold nanoparticles. According to the authors, this conclusion implies that optical sensors relying on the desorption of aptamers from Au NPs due to target binding can be inaccurate and should be avoided [51]. Even though their method was thoroughly detailed, their conclusion shouldn't be generalized for all optical sensors for several reasons. While it is true that the interaction between gold nanoparticles and DNA is strong, it can be affected by factors such as the pH, ionic strength, the nucleobases involved in the sequence and its length, and the interaction between the nucleobases and the different possible target molecules. Nonetheless, not all those factors were studied in the mentioned paper, and thus further investigations should be done to take into consideration the remaining factors. Recently, a lot of the developed optical sensors do not rely on the desorption of the aptamer sequence from Au NPs for detection, but rather on the change in color of the nanoparticles in presence/absence of the aptamer and target. Qi et al. even used a control aptamer with a random sequence to confirm the efficiency of the design of their sensor [52].

Less commonly, a few studies have attempted the detection of lead and mercury using quartz crystal microbalance (QCM), magnetic relaxation switching (MRS) and chemiluminescence (CL). Generally, it can be noticed that the limits of detection obtained using non-electrochemical methods were mostly higher than those obtained with electrochemical techniques.

The proposed sensors were tested in real samples such as water [1, 3, 12, 20, 22, 25, 26, 29-31, 33, 37-39, 41, 45-49, 52, 56-73, 75], wastewater [23, 24, 33, 57, 61], cosmetics [39] baby nail [55], serum [28, 31], soil [12, 35, 55, 68], milk [34, 46, 49], fish [25, 27], tea [23], herbs [21], wine [10, 76] and rice [37]. Almost half of those sensors were tested for their reproducibility [1, 3, 24, 26, 27, 30, 31, 33-35, 48, 49, 54, 55, 56-64] in which the response of at least 4 sensors was investigated and the relative standard deviation was between 1.87% and 7.8%. On the other hand, only a few were examined for possible reusability [1, 31, 32, 56, 57, 64, 66]. The reproducibility was acceptable to excellent, and most sensors could be used at least three times before the signal starts changing.

Table 2 Non-electrochemical aptasensors using gold nanoparticles for the detection of heavy metals

3.2.Other Metallic Nanoparticles

Silver Ag and platinum Pt are among the metal nanoparticles that have been combined with aptamers for the detection of heavy metal ions. In addition to the advantages of good electrical conductivity and large surface area, these nanoparticles also have a favorable catalytic activity in a wide range of pH and temperature conditions.

Jin et al. developed a lead electrochemical aptasensor based on biomass porous carbon derived from soybean straws, platinum nanoparticles and several DNA strands: 5'-GGG TGG GTG GGT GGG TAT-3', complementary DNA: 5'-TCA TAC CCA CCC ACC-3', hairpin DNA 1: 5'-TTT TGG GTG GGT ATG ACC ACC GCC CAC CCA-3' and Bio-Hairpin DNA 2: 5'-bio-TAT GAC CAC CTG GGT GGG CGG TGG TCA TAC CCA C-3'. The biosensor exhibited a

linear range of 50 pM – 1000 nM with a detection limit of 18 pM. The proposed sensor was also successfully tested in tap water and lake water [9].

Song et al. proposed a portable ultrasensitive SERS sensor based on T-rich oligonucleotides 5′-thiol-TTTTTTTTTTTTTTT-Cy5-3′ immobilized on silver nanorods for the detection of mercury (II) ions. The mercury – thymine interaction led to a change in structure of the DNA and hence in the SERS signal. A linear range was obtained between 1 pM and 1 μM with a detection limit of 0.16 pM. Good recovery rates were also obtained upon testing the sensor in tap and lake water [53].

Bimetallic AgPt nanoparticles can significantly increase the surface area and have good electrical conductivity and electrocatalytic activity. Xu et al. designed an electrochemical aptasensor for the detection of lead ions. The biosensor was made using metal-organic frameworks decorated with AgPt nanoparticles conjugated with single stranded DNA 3'-NH_2-$(CH_2)_6$-CCCACCCACC-5' complementary to a guanine-rich lead specific aptamer 5'-GGGTGGGTGGGTGGGT-$(CH_2)_6$-NH_2-3'. The developed sensor showed a linear response in the concentration range of 0.1 pM and 100 nM as well as a detection limit of 0.032 pM with potential application in tap and lake water [50] (figure 2d).

As can be seen, electrochemical and optical biosensors were developed using silver and platinum nanoparticles for the detection of lead and mercury. Compared with the results obtained using gold nanoparticles reported in this review, the LODs obtained with Ag and Pt electrochemical sensors were not as low, which might explain the humble number of articles using these nanoparticles recently. On the other hand, the performance of the optical sensors is comparable to those using gold nanoparticles. Most of those sensors were evaluated for their reproducibility, which was acceptable, but none for their reusability.

4. Metal oxide nanoparticles

Some metal oxide nanoparticles such as ZnO, CuO, Fe_3O_4, SnO_2, TiO_2 and MnO_2 have been widely explored for the identification and detection of heavy metal ions because of their non-toxic and catalytic properties. Magnetic nanoparticles have received considerable attention due to their low toxicity, ease of preparation and biocompatibility [3]. Metal oxide nanoparticles offer the advantages of significant electron transfer kinetics and large specific area thus possessing a large number of adsorption sites.

Even though Fe_3O_4 nanoparticles are the most common form of metal oxide nanoparticles used for the detection of heavy metal ions, some studies have used Co_3O_4, TiO_2 and CeO_2 nanoparticles (table 3). The development of the above biosensors and detection mechanisms are similar to those with gold nanoparticles. However, the limits of detection obtained were not as low as those obtained with gold nanoparticles.

Interestingly, only around 50% of the studies mentioned in this section have reported an "acceptable" to "excellent" reproducibility [3, 25, 11, 77, 81, 82] by studying the response of their proposed sensors at least three times with relative standard deviation ranging between 4.3% and 8.8%. Almost all those studies have reported the use of their sensors in real samples such as water [2, 3, 11, 25, 65, 79-81, 83], human blood [77, 82], urine [82], soil [78], fish [25, 80] and wine [10]. Only one study reported the reuse of their sensor up to 8 times [82].

Since most studies aim at analyzing mercury ions, the different reports using Fe_3O_4 nanoparticles for the detection of mercury can be compared in figure 3. The number of studies relying on iron oxide nanoparticles is insignificant compared to those using gold nanoparticles. Thus, we can say that the numerous possibilities of detection have not yet been explored.

Nevertheless, an exceptionally low limit of detection of 2 aM was obtained electrochemically, proving that iron oxide nanoparticles can be considered as competitors for gold nanoparticles.

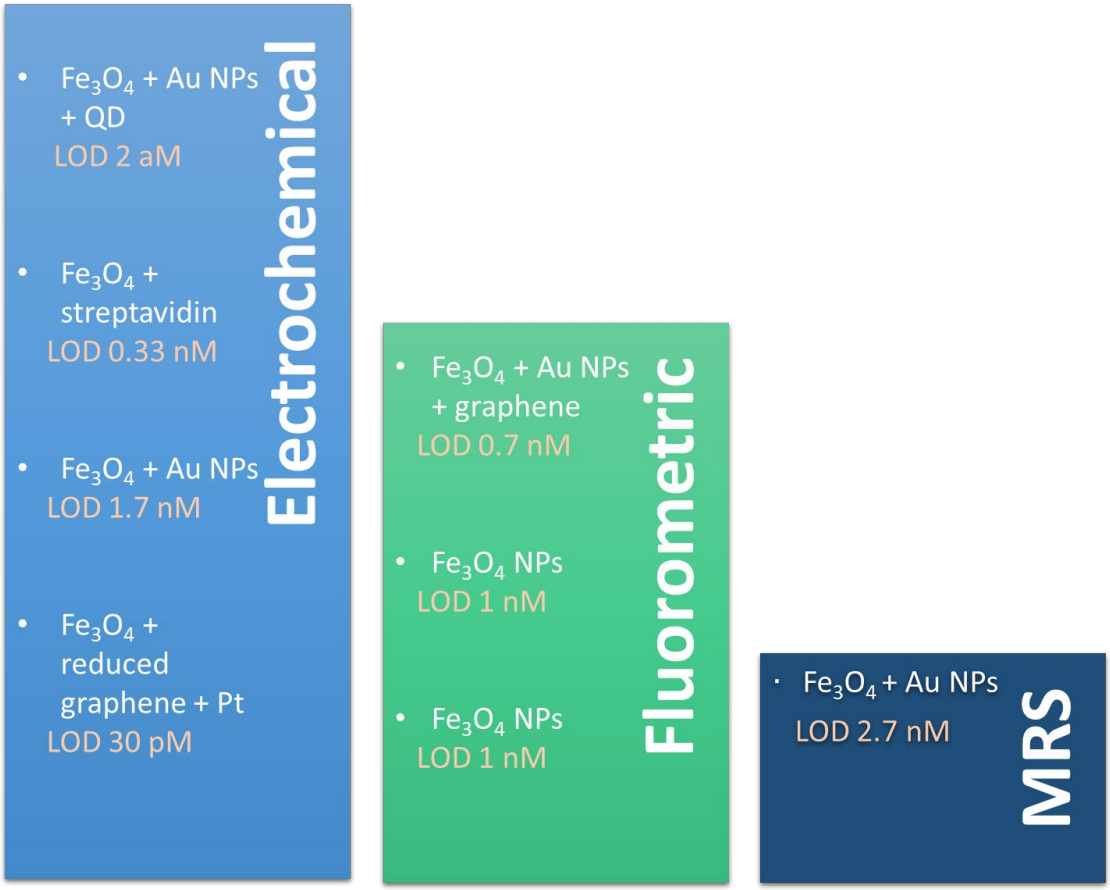

Figure 3: Comparison of the thymine aptamer-based techniques for the detection of mercury ions

5. Summary and perspectives

Aptamer-based technologies have been developed as effective sensing tools for various analytes. To the best of our knowledge, there hasn't been an update on heavy metal monitoring based on aptamers using nanoparticles in the past few years. Hence, this review presents the most recent metallic and metallic oxide nanoparticles combined with aptamer-based approaches for the monitoring of arsenic, cadmium, copper, lead, mercury, silver and platinum in various samples. It has been known that the affinity and specificity of aptamers towards their analytes are the main

advantages supporting their use. Nonetheless, the advantages of nanoparticles and aptamers, as well as the new properties that result from combining the two technologies all contributed to enhance analytical performances of the proposed methods, which can be evident by comparing the LODs and linear ranges with those obtained using aptamer-free sensors presented in recent reviews [84]. The main mechanisms involved in the presence of heavy metals are:

- the dehybridization of capture DNA and specific aptamer and the release of the intercalating agent
- the hindering of the interaction of the specific aptamer with a cationic polymer (ex. PDDA)
- the formation of the G-quadruplex with the specific aptamer
- the formation of the rigid hairpin-shaped double-stranded DNA

In the case of Hg^{2+} ion, the thymine-Hg2+-thymine coordination induces the formation of a DNA duplex or of an hairpin duplex.

Even though gold nanoparticles are the most commonly used with aptamers for the detection of heavy metal ions reporting extremely low detection limits, several other nanoparticles have emerged as promising modifications to aptamers in heavy metal monitoring as well. Comparing the different techniques used, electrochemical methods have presented the best performance while offering their advantages over optical and spectrometric techniques. Moreover, only mercury has been broadly examined using non-electrochemical techniques to obtain a good analytical performance. On the other hand, studies using electrochemical methods have reached optimum analytical performance for more than one heavy metal ion (mercury, lead, arsenic).

Despite all that, each proposed system was at best applied to one or a few environmental, food or biological samples in order to test its applicability in sensing the specific heavy metal. Nevertheless, these matrices usually contain more than one heavy metal along with other organic and inorganic compounds. While a few sensors were tested for interferences, complex matrices would probably require further modifications and improvements to the developed sensors. Besides, reusability of the sensors remains a challenge since it was not addressed in most of the studies in this review. It is worth noting that the use of different nanomaterials such as quantum dots along with the nanoparticles, or even the use of bimetallic nanoparticles are proving to be promising in this field. Thus, we anticipate significant progress in developing novel aptamer-based sensors using various nanomaterials in the future.

References

[1] Y. Zhao, X. Xie, A Novel Electrochemical Aptamer Biosensor Based on DNAzyme Decorated Au@Ag Core-Shell Nanoparticles for Hg2+ Determination, J. Braz. Chem. Soc., 29 (2017) 232-239. https://doi.org/10.21577/0103-5053.20170133

[2] Y. Shan, B. Wang, H. Huang, D. Jian, X. Wu, L. Xue, S. Wang, F. Liu, On-site quantitative Hg(2+) measurements based on selective and sensitive fluorescence biosensor and miniaturized smartphone fluorescence microscope, Biosens. Bioelectron., 132 (2019) 238-247. https://doi.org/10.1016/j.bios.2019.02.062

[3] P. Miao, Y. Tang, L. Wang, DNA Modified Fe3O4@Au Magnetic Nanoparticles as Selective Probes for Simultaneous Detection of Heavy Metal Ions, ACS Appl. Mater. Interfaces, 9 (2017) 3940-3947. https://doi.org/10.1021/acsami.6b14247

[4] M. Mittal, K. Kumar, D. Anghore, R. K Rawal, ICP-MS: Analytical method for identification and detection of elemental impurities, Curr. Drug Discovery Technol., 14 (2017) 106-120. https://doi.org/10.2174/1570163813666161221141402

[5] G. Heltai, Z. Győri, I. Fekete, G. Halász, K. Kovács, A. Takács, L. Khumalo, M. Horváth, Application of flexible multi-elemental ICP-OES detection in fractionation of potentially toxic element content of solid environmental samples by a sequential extraction procedure, Microchem. J., 149 (2019) 104029. https://doi.org/10.1016/j.microc.2019.104029

[6] F. Pan, Y. Yu, L. Yu, H. Lin, Y. Wang, L. Zhang, D. Pan, R. Zhu, Quantitative assessment on soil concentration of heavy metal–contaminated soil with various sample pretreatment techniques and detection methods, Environ. Monit. Assess. , 192 (2020) 1-8. https://doi.org/10.1007/s10661-020-08775-4

[7] S. Akram, R. Najam, G.H. Rizwani, S.A. Abbas, Determination of heavy metal contents by atomic absorption spectroscopy (AAS) in some medicinal plants from Pakistani and Malaysian origin, Pak. J. Pharm. Sci., 28 (2015)

[8] P.R. Aranda, P.H. Pacheco, R.A. Olsina, L.D. Martinez, R.A. Gil, Total and inorganic mercury determination in biodiesel by emulsion sample introduction and FI-CV-AFS after multivariate optimization, J. Anal. At. Spectrom., 24 (2009) 1441-1445. https://doi.org/10.1039/B903113H

[9] H. Jin, D. Zhang, Y. Liu, M. Wei, An electrochemical aptasensor for lead ion detection based on catalytic hairpin assembly and porous carbon supported platinum as signal amplification, RSC Advances, 10 (2020) 6647-6653. https://doi.org/10.1039/d0ra00022a

[10] Z. Tao, Y. Zhou, N. Duan, Z. Wang, A Colorimetric Aptamer Sensor Based onthe Enhanced Peroxidase Activity of FunctionalizedGrapheneFe3O4-AuNPs for Detection ofLead (II) Ions, Catalysts 10 (2020) 600. https://doi.org/10.3390/catal10060600

[11] Y. Liu, D. Zhang, J. Ding, K. Hayat, X. Yang, X. Zhan, D. Zhang, Y. Lu, P. Zhou, Label-Free and Sensitive Determination of Cadmium Ions Using a Ti-Modified Co3O4-Based Electrochemical Aptasensor, Biosensors (Basel), 10 (2020) 195. https://doi.org/10.3390/bios10120195

[12] S. Xu, X. Chen, G. Peng, L. Jiang, H. Huang, An electrochemical biosensor for the detection of Pb(2+) based on G-quadruplex DNA and gold nanoparticles, Anal Bioanal Chem, 410 (2018) 5879-5887. https://doi.org/10.1007/s00216-018-1204-6

[13] S. Sahin, M.O. Caglayan, Z. Ustundag, A review on nanostructure-based mercury (II) detection and monitoring focusing on aptamer and oligonucleotide biosensors, Talanta, 220 (2020) 121437. https://doi.org/10.1016/j.talanta.2020.121437

[14] S. Dolati, M. Ramezani, K. Abnous, S.M. Taghdisi, Recent nucleic acid based biosensors for Pb2+ detection, Sens. Actuators, B, 246 (2017) 864-878. https://doi.org/10.1016/j.snb.2017.02.118

[15] K. Mao, H. Zhang, Z. Wang, H. Cao, K. Zhang, X. Li, Z. Yang, Nanomaterial-based aptamer sensors for arsenic detection, Biosens. Bioelectron., 148 (2020) 111785. https://doi.org/10.1016/j.bios.2019.111785

[16] M.A. Deshmukh, M.D. Shirsat, A. Ramanaviciene, A. Ramanavicius, Composites Based on Conducting Polymers and Carbon Nanomaterials for Heavy Metal Ion Sensing (Review), Crit. Rev. Anal. Chem., 48 (2018) 293-304. https://doi.org/10.1080/10408347.2017.1422966

[17] N. Ullah, M. Mansha, I. Khan, A. Qurashi, Nanomaterial-based optical chemical sensors for the detection of heavy metals in water: Recent advances and challenges, TrAC Trends Anal. Chem., 100 (2018) 155-166. https://doi.org/10.1016/j.trac.2018.01.002

[18] W. Zhou, R. Saran, J. Liu, Metal Sensing by DNA, Chem. Rev., 117 (2017) 8272-8325. https://doi.org/10.1021/acs.chemrev.7b00063

[19] R.K.O. Sigel, H. Sigel, A Stability Concept for Metal Ion Coordination to Single-Stranded Nucleic Acids and Affinities of Individual Sites, Acc. Chem. Res., 43 (2010) 974-984. https://doi.org/10.1021/ar900197y

[20] M. Zhou, T. Lin, X. Gan, Colorimetric aggregation assay for silver(I) based on the use of aptamer modified gold nanoparticles and C-Ag(I)-C interaction, Microchim. Acta, 184 (2017) 4671-4677. https://doi.org/10.1007/s00604-017-2518-3

[21] L.-L. He, L. Cheng, Y. Lin, H.-F. Cui, N. Hong, H. Peng, D.-R. Kong, C.-D. Chen, J. Zhang, G.-B. Wei, H. Fan, A sensitive biosensor for mercury ions detection based on hairpin hindrance by thymine-Hg(II)-thymine structure, J. Electroanal. Chem., 814 (2018) 161-167. https://doi.org/10.1016/j.jelechem.2018.02.050

[22] W. Tang, J. Yu, Z. Wang, I. Jeerapan, L. Yin, F. Zhang, P. He, Label-free potentiometric aptasensing platform for the detection of Pb(2+) based on guanine quadruplex structure, Anal. Chim. Acta, 1078 (2019) 53-59. https://doi.org/10.1016/j.aca.2019.06.020

[23] M. Chen, M. Hassan, H. Li, Q. Chen, Fluorometric determination of lead(II) by using aptamer-functionalized upconversion nanoparticles and magnetite-modified gold nanoparticles, Microchim. Acta, 187 (2020) 85. https://doi.org/10.1007/s00604-019-4030-4

[24] A.T. Ezhil Vilian, A. Shahzad, J. Chung, S.R. Choe, W.-S. Kim, Y.S. Huh, T. Yu, Y.-K. Han, Square voltammetric sensing of mercury at very low working potential by using oligomer-

functionalized Ag@Au core-shell nanoparticles, Microchim. Acta, 184 (2017) 3547-3556. https://doi.org/10.1007/s00604-017-2372-3

[25] B. Babamiri, A. Salimi, R. Hallaj, Switchable electrochemiluminescence aptasensor coupled with resonance energy transfer for selective attomolar detection of Hg(2+) via CdTe@CdS/dendrimer probe and Au nanoparticle quencher, Biosens. Bioelectron., 102 (2018) 328-335. https://doi.org/10.1016/j.bios.2017.11.034

[26] X. Fan, S. Wang, Z. Li, Y. Wang, X. Fan, L. Yu, An Electrochemiluminescence Biosensor for the Determination of Mercury Ion via Dual-Amplification Strategy, J. Braz. Chem. Soc., 31 (2020) 2620-2627. https://doi.org/10.21577/0103-5053.20200144

[27] D. Feng, P. Li, X. Tan, Y. Wu, F. Wei, F. Du, C. Ai, Y. Luo, Q. Chen, H. Han, Electrochemiluminescence aptasensor for multiple determination of Hg(2+) and Pb(2+) ions by using the MIL-53(Al)@CdTe-PEI modified electrode, Anal. Chim. Acta, 1100 (2020) 232-239. https://doi.org/10.1016/j.aca.2019.11.069

[28] C. Wang, M. Chen, J. Wu, F. Mo, Y. Fu, Multi-functional electrochemiluminescence aptasensor based on resonance energy transfer between Au nanoparticles and lanthanum ion-doped cadmium sulfide quantum dots, Anal. Chim. Acta, 1086 (2019) 66-74. https://doi.org/10.1016/j.aca.2019.08.012

[29] D.M. Wang, Q.Q. Gai, R.F. Huang, X. Zheng, Label-free electrochemiluminescence assay for aqueous Hg(2+) through oligonucleotide mediated assembly of gold nanoparticles, Biosens. Bioelectron., 98 (2017) 134-139. https://doi.org/10.1016/j.bios.2017.06.054

[30] Y. Peng, Y. Li, L. Li, J.J. Zhu, A label-free aptasensor for ultrasensitive Pb(2+) detection based on electrochemiluminescence resonance energy transfer between carbon nitride nanofibers

and Ru(phen)3(2), J. Hazard. Mater., 359 (2018) 121-128. https://doi.org/10.1016/j.jhazmat.2018.07.033

[31] Y. Wang, G. Zhao, Q. Zhang, H. Wang, Y. Zhang, W. Cao, N. Zhang, B. Du, Q. Wei, Electrochemical aptasensor based on gold modified graphene nanocomposite with different morphologies for ultrasensitive detection of Pb2+, Sens. Actuators, B, 288 (2019) 325-331. https://doi.org/10.1016/j.snb.2019.03.010

[32] G. Zhao, C. Li, X. Wang, G. Liu, N.T.D. Thuy, A Reusable Electrochemical Aptasensor for the Sensitive Detection of Pb(II) with an Electrodeposited AuNP-Modified Electrode based on the Formation of a Target-Induced G- Quadruplex, Int. J. Electrochem. Sci., 16 (2021) 150956. https://doi.org/10.20964/2021.01.09

[33] A.A. Ensafi, F. Akbarian, E. Heydari-Soureshjani, B. Rezaei, A novel aptasensor based on 3D-reduced graphene oxide modified gold nanoparticles for determination of arsenite, Biosens. Bioelectron., 122 (2018) 25-31. https://doi.org/10.1016/j.bios.2018.09.034

[34] X. Zhang, C. Huang, Y. Jiang, Y. Jiang, J. Shen, E. Han, Structure-Switching Electrochemical Aptasensor for Single-Step and Specific Detection of Trace Mercury in Dairy Products, J. Agric. Food Chem., 66 (2018) 10106-10112. https://doi.org/10.1021/acs.jafc.8b03259

[35] J. Ding, D. Zhang, Y. Liu, M. Yu, X. Zhan, D. Zhang, P. Zhou, An electrochemical aptasensor for detection of lead ions using a screen-printed carbon electrode modified with Au/polypyrrole composites and toluidine blue, Anal. Methods, 11 (2019) 4274-4279. https://doi.org/10.1039/c9ay01256g

[36] X. Liu, Z. Wu, Q. Zhang, W. Zhao, C. Zong, H. Gai, Single Gold Nanoparticle-Based Colorimetric Detection of Picomolar Mercury Ion with Dark-Field Microscopy, Anal. Chem., 88 (2016) 2119-2124. https://doi.org/10.1021/acs.analchem.5b03653

[37] L. Xu, J. Liang, Y. Wang, S. Ren, J. Wu, H. Zhou, Z. Gao, Highly Selective, Aptamer-Based, Ultrasensitive Nanogold Colorimetric Smartphone Readout for Detection of Cd(II), Molecules, 24 (2019) 2745. https://doi.org/10.3390/molecules24152745

[38] K. Matsunaga, Y. Okuyama, R. Hirano, S. Okabe, M. Takahashi, H. Satoh, Development of a simple analytical method to determine arsenite using a DNA aptamer and gold nanoparticles, Chemosphere, 224 (2019) 538-543. https://doi.org/10.1016/j.chemosphere.2019.02.182

[39] N.L. Thao Nguyen, C.Y. Park, J.P. Park, S.K. Kailasa, T.J. Park, Synergistic molecular assembly of an aptamer and surfactant on gold nanoparticles for the colorimetric detection of trace levels of As3+ ions in real samples, New J. Chem., 42 (2018) 11530-11538. https://doi.org/10.1039/c8nj01097h

[40] C. Zong, J. Liu, The Arsenic-Binding Aptamer Cannot Bind Arsenic: Critical Evaluation of Aptamer Selection and Binding, Anal. Chem., 91 (2019) 10887-10893. https://doi.org/10.1021/acs.analchem.9b02789

[41] D. Zhang, Y. Liu, J. Ding, K. Hayat, X. Zhan, P. Zhou, D. Zhang, Label-free colorimetric assay for arsenic(III) determination based on a truncated short ssDNA and gold nanoparticles, Microchim. Acta, 188 (2021) 38. https://doi.org/10.1007/s00604-020-04697-7

[42] Y. Hu, Z. Huang, B. Liu, J. Liu, Hg(II) Adsorption on Gold Nanoparticles Dominates DNA-Based Label-Free Colorimetric Sensing, ACS Applied Nano Materials, 4 (2021) 1377-1384. https://doi.org/10.1021/acsanm.0c02923

[43] X. Niu, Y. Zhong, R. Chen, F. Wang, Y. Liu, D. Luo, A “turn-on” fluorescence sensor for Pb2+ detection based on graphene quantum dots and gold nanoparticles, Sens. Actuators, B, 255 (2018) 1577-1581. https://doi.org/10.1016/j.snb.2017.08.167

[44] Y. Wang, M. Lv, Z. Chen, Z. Deng, N. Liu, J. Fan, W. Zhang, A Fluorescence Resonance Energy Transfer Probe Based on DNA-Modified Upconversion and Gold Nanoparticles for Detection of Lead Ions, Front. Chem., 8 (2020) 238. https://doi.org/10.3389/fchem.2020.00238

[45] Z. Wu, H. Shen, J. Hu, Q. Fu, C. Yao, S. Yu, W. Xiao, Y. Tang, Aptamer-based fluorescence-quenching lateral flow strip for rapid detection of mercury (II) ion in water samples, Anal. Bioanal. Chem., 409 (2017) 5209-5216. https://doi.org/10.1007/s00216-017-0491-7

[46] Y. Liu, Q. Ouyang, H. Li, M. Chen, Z. Zhang, Q. Chen, Turn-On Fluoresence Sensor for Hg(2+) in Food Based on FRET between Aptamers-Functionalized Upconversion Nanoparticles and Gold Nanoparticles, J. Agric. Food Chem., 66 (2018) 6188-6195. https://doi.org/10.1021/acs.jafc.8b00546

[47] H. Ouyang, S. Ling, A. Liang, Z. Jiang, A facile aptamer-regulating gold nanoplasmonic SERS detection strategy for trace lead ions, Sens. Actuators, B, 258 (2018) 739-744. https://doi.org/10.1016/j.snb.2017.12.009

[48] Y. Lu, J. Zhong, G. Yao, Q. Huang, A label-free SERS approach to quantitative and selective detection of mercury (II) based on DNA aptamer-modified SiO2@Au core/shell nanoparticles, Sens. Actuators, B, 258 (2018) 365-372. https://doi.org/10.1016/j.snb.2017.11.110

[49] Y. Wu, T. Jiang, Z. Wu, R. Yu, Novel ratiometric surface-enhanced raman spectroscopy aptasensor for sensitive and reproducible sensing of Hg(2), Biosens. Bioelectron., 99 (2018) 646-652. https://doi.org/10.1016/j.bios.2017.08.041

[50] W. Xu, X. Zhou, J. Gao, S. Xue, J. Zhao, Label-free and enzyme-free strategy for sensitive electrochemical lead aptasensor by using metal-organic frameworks loaded with AgPt nanoparticles as signal probes and electrocatalytic enhancers, Electrochim. Acta, 251 (2017) 25-31. https://doi.org/10.1016/j.electacta.2017.08.046

[51] F. Zhang, S. Wang, J. Liu, Gold Nanoparticles Adsorb DNA and Aptamer Probes Too Strongly and a Comparison with Graphene Oxide for Biosensing, Anal. Chem., 91 (2019) 14743-14750. https://doi.org/10.1021/acs.analchem.9b04142

[52] Y. Qi, J. Ma, X. Chen, F.R. Xiu, Y. Chen, Y. Lu, Practical aptamer-based assay of heavy metal mercury ion in contaminated environmental samples: convenience and sensitivity, Anal. Bioanal. Chem., 412 (2020) 439-448. https://doi.org/10.1007/s00216-019-02253-8

[53] C. Song, B. Yang, Y. Zhu, Y. Yang, L. Wang, Ultrasensitive sliver nanorods array SERS sensor for mercury ions, Biosens. Bioelectron., 87 (2017) 59-65. https://doi.org/10.1016/j.bios.2016.07.097

[54] M. Adabi, Detection of lead ions using an electrochemical aptasensor, Nanomed. Res. J., 4(2019) 247-252. https://doi.org/10.22034/nmrj.2019.04.007

[55] J. Ding, Y. Liu, D. Zhang, M. Yu, X. Zhan, D. Zhang, P. Zhou, An electrochemical aptasensor based on gold@polypyrrole composites for detection of lead ions, Microchim. Acta, 185 (2018) 545. https://doi.org/10.1007/s00604-018-3068-z

[56] Y. Zhang, C. Zhang, R. Ma, X. Du, W. Dong, Y. Chen, Q. Chen, An ultra-sensitive Au nanoparticles functionalized DNA biosensor for electrochemical sensing of mercury ions, Mater. Sci. Eng. B, 75 (2017) 175-181. https://doi.org/10.1016/j.msec.2017.02.058

[57] H. Jin, M. Zhang, M. Wei, J.H. Cheng, A voltammetric biosensor for mercury(II) using reduced graphene oxide@gold nanorods and thymine-Hg(II)-thymine interaction, Microchim. Acta, 186 (2019) 264. https://doi.org/10.1007/s00604-019-3372-2

[58] A. Mohammadi, E. Heydari-Bafrooei, M.M. Foroughi, M. Mohammadi, Heterostructured Au/MoS2-MWCNT nanoflowers: A highly efficient support for the electrochemical aptasensing

of solvated mercuric ion, Microchem. J., 158 (2020). https://doi.org/10.1016/j.microc.2020.105154

[59] L. Zhao, Y. Wang, G. Zhao, N. Zhang, Y. Zhang, X. Luo, B. Du, Q. Wei, Electrochemical aptasensor based on Au@HS-rGO and thymine-Hg2+-thymine structure for sensitive detection of mercury ion, Journal of Electroanalytical Chemistry, 848 (2019) 113308.https://doi.org/10.1016/j.jelechem.2019.113308

[60] Y. Shi, G. Zhang, J. Li, Y. Zhang, Y. Yu, Q. Wei, Photoelectrochemical determination of Hg(II) via dual signal amplification involving SPR enhancement and a folding-based DNA probe, Microchim. Acta, 184 (2017) 1379-1387. https://doi.org/10.1007/s00604-017-2141-3

[61] T. Mushiana, N. Mabuba, A.O. Idris, G.M. Peleyeju, B.O. Orimolade, D. Nkosi, R.F. Ajayi, O.A. Arotiba, An aptasensor for arsenic on a carbon-gold bi-nanoparticle platform, Sensing and Bio-Sensing Research, 24 (2019) 100280. https://doi.org/10.1016/j.sbsr.2019.100280

[62] C.T. Fakude, O.A. Arotiba, N. Mabuba, Electrochemical aptasensing of cadmium (II) on a carbon black-gold nano-platform, J. Electroanal. Chem., 858 (2020) 113796. https://doi.org/10.1016/j.jelechem.2019.113796

[63] Y. Liu, Y. Lai, G. Yang, C. Tang, Y. Deng, S. Li, Z. Wang, Cd-Aptamer Electrochemical Biosensor Based on AuNPs/CS Modified Glass Carbon Electrode, J. Biomed. Nanotechnol., 13 (2017) 1253-1259. https://doi.org/10.1166/jbn.2017.2424

[64] M. Yuan, Z. Song, J. Fei, X. Wang, F. Xu, H. Cao, J. Yu, Aptasensor for lead(II) based on the use of a quartz crystal microbalance modified with gold nanoparticles, Microchim. Acta, 184 (2017) 1397-1403. https://doi.org/10.1007/s00604-017-2135-1

[65] Y. Liu, Z. Cai, L. Sheng, M. Ma, X. Wang, A magnetic relaxation switching and visual dual-mode sensor for selective detection of Hg(2+) based on aptamers modified Au@Fe3O4

nanoparticles, J. Hazard. Mater., 388 (2020) 121728. https://doi.org/10.1016/j.jhazmat.2019.121728

[66] S. Jia, C. Bian, J. Sun, J. Tong, S. Xia, A wavelength-modulated localized surface plasmon resonance (LSPR) optical fiber sensor for sensitive detection of mercury(II) ion by gold nanoparticles-DNA conjugates, Biosens. Bioelectron., 114 (2018) 15-21. https://doi.org/10.1016/j.bios.2018.05.004

[67] Y. Qi, F.R. Xiu, G. Yu, L. Huang, B. Li, Simple and rapid chemiluminescence aptasensor for Hg(2+) in contaminated samples: A new signal amplification mechanism, Biosens. Bioelectron., 87 (2017) 439-446. https://doi.org/10.1016/j.bios.2016.08.022

[68] H.-B. Wang, L.-H. Ma, B.-Y. Fang, F. Tan, Y.-C. Cao, Y.-D. Zhao, X.-B. Hu, Visual detection of Pb2+ using strip biosensor based on PS2M aptamer and sensitivity enhancement probe, Sens. Actuators, B, 261 (2018) 307-315. https://doi.org/10.1016/j.snb.2018.01.167

[69] S. Sajed, M. Kolahdouz, M.A. Sadeghi, S.F. Razavi, High-Performance Estimation of Lead Ion Concentration Using Smartphone-Based Colorimetric Analysis and a Machine Learning Approach, ACS Omega, 5 (2020) 27675-27684. https://doi.org/10.1021/acsomega.0c04255

[70] D. Wang, C. Ge, K. Lv, Q. Zou, Q. Liu, L. Liu, Q. Yang, S. Bao, A simple lateral flow biosensor for rapid detection of lead(ii) ions based on G-quadruplex structure-switching, Chem. Commun. (Camb), 54 (2018) 13718-13721. https://doi.org/10.1039/c8cc06810k

[71] A.N. Berlina, A.V. Zherdev, S.M. Pridvorova, M.S. Gaur, B.B. Dzantiev, Rapid Visual Detection of Lead and Mercury via Enhanced Crosslinking Aggregation of Aptamer-Labeled Gold Nanoparticles, J. Nanosci. Nanotechnol., 19 (2019) 5489-5495. https://doi.org/10.1166/jnn.2019.16575

[72] L. Tan, Z. Chen, C. Zhang, X. Wei, T. Lou, Y. Zhao, Colorimetric Detection of Hg(2+) Based on the Growth of Aptamer-Coated AuNPs: The Effect of Prolonging Aptamer Strands, Small, 13 (2017) 1603370. https://doi.org/10.1002/smll.201603370

[73] X. Song, Y. Wang, S. Liu, X. Zhang, H. Wang, J. Wang, J. Huang, Colorimetric and visual mercury(II) assay based on target-induced cyclic enzymatic amplification, thymine-Hg(II)-thymine interaction, and aggregation of gold nanoparticles, Microchim. Acta, 186 (2019) 105. https://doi.org/10.1007/s00604-018-3193-8

[74] A.G. Memon, X. Zhou, J. Liu, R. Wang, L. Liu, B. Yu, M. He, H. Shi, Utilization of unmodified gold nanoparticles for label-free detection of mercury (II): Insight into rational design of mercury-specific oligonucleotides, J. Hazard. Mater., 321 (2017) 417-423. https://doi.org/10.1016/j.jhazmat.2016.09.025

[75] Y. Gan, T. Liang, Q. Hu, L. Zhong, X. Wang, H. Wan, P. Wang, In-situ detection of cadmium with aptamer functionalized gold nanoparticles based on smartphone-based colorimetric system, Talanta, 208 (2020) 120231. https://doi.org/10.1016/j.talanta.2019.120231

[76] Z. Tao, L. Wei, S. Wu, N. Duan, X. Li, Z. Wang, A colorimetric aptamer-based method for detection of cadmium using the enhanced peroxidase-like activity of Au-MoS2 nanocomposites, Anal. Biochem., 608 (2020) 113844. https://doi.org/10.1016/j.ab.2020.113844

[77] Y. Song, C. Guo, H. Ji, S. Zhang, M. Wang, L. He, D. Peng, Z. Zhang, Cu x O@DNA sphere-based electrochemical bioassay for sensitive detection of Pb(2), Microchim. Acta, 185 (2018) 186. https://doi.org/10.1007/s00604-018-2729-2

[78] Y. Niu, G. Luo, H. Xie, Y. Zhuang, X. Wu, G. Li, W. Sun, Photoelectrochemical aptasensor for lead(II) by exploiting the CdS nanoparticle-assisted photoactivity of TiO2 nanoparticles and

by using the quercetin-copper(II) complex as the DNA intercalator, Microchim. Acta, 186 (2019) 826. https://doi.org/10.1007/s00604-019-3951-2

[79] L. Yang, B. An, X. Yin, F. Li, A competitive coordination-based immobilization-free electrochemical biosensor for highly sensitive detection of arsenic(v) using a CeO2-DNA nanoprobe, Chem. Commun. (Camb), 56 (2020) 5311-5314. https://doi.org/10.1039/d0cc01821j

[80] C. Sun, R. Sun, Y. Chen, Y. Tong, J. Zhu, H. Bai, S. Zhang, H. Zheng, H. Ye, Utilization of aptamer-functionalized magnetic beads for highly accurate fluorescent detection of mercury (II) in environment and food, Sens. Actuators, B, 255 (2018) 775-780. https://doi.org/10.1016/j.snb.2017.08.004

[81] J. Luo, D. Jiang, T. Liu, J. Peng, Z. Chu, W. Jin, High-performance electrochemical mercury aptasensor based on synergistic amplification of Pt nanotube arrays and Fe3O4/rGO nanoprobes, Biosens. Bioelectron., 104 (2018) 1-7. https://doi.org/10.1016/j.bios.2017.12.044

[82] M. Shamsipur, L. Farzin, M.A. Tabrizi, S. Sheibani, Functionalized Fe3O4 graphene oxide nanocomposites with hairpinaptamers for the separation and preconcentration of trace Pb2+frombiological samples prior to determination by ICP MS, Mater. Sci. Eng. C., 77 (2017) 459–469. https://doi.org/10.1016/j.msec.2017.03.262

[83] S. Rahnama, S. Shariati, F. Divsar, Selective aptamer conjugation to silver-coated magnetite nanoparticles for magnetic solid-phase extraction of trace amounts of Pb2+ ions, RSC Advances, 11 (2021) 4971-4982. https://doi.org/10.1039/d1ra00006c

[84] S. Sawan, R. Maalouf, A. Errachid, N. Jaffrezic-Renault, Metal and metal oxide nanoparticles in the voltammetric detection of heavy metals: A review, TrAC Trends in Analytical Chemistry, 131 (2020) 116014. https://doi.org/10.1016/j.trac.2020.116014

Table 1 Electrochemical aptasensors using gold nanoparticles for the detection of heavy metals

Modification	Aptamer	Technique	Heavy metal	LOD (nM)	Linear range (nM)	Operational conditions	Ref
Au NPs	5′-CACCCACCCAC-$(CH_2)_6$-SH-3 ′; 5′-GGGTGGGTGGGTGGGT-3	Chronocoulometry	Pb^{2+}	4.2×10^{-3}	0.01 – 200	Ph 7.4	[12]
Au NPs	5’-TGGGTGGGTGGGTGGG-3’; 5’-NH_2-CCCACCCACCCTTTTT-3’; 5’-NH_2-CCCACCCACCCACCCA-3’; 5’-NH_2-CCCACCCACCCATTTT-3’; 5’-NH_2-CCCACCCACCCTTTTT-3’; 5’-NH_2-CCCACCCACCTTTTTT-3’; 5’-NH_2-CCCACCCACTTTTTTT-3’; 5’-NH_2-CCCACCCATTTTTTTT-3’; 5’- AAAAATGGGTGTGA-3’	EIS	Pb^{2+}	0.0046	4.83 – 480	$K_3[Fe(CN)_6]$ (0.1 mM), 10 mM PBS pH 7.4	[32]

Au NPs-thionine	5’-GGGTGGGTGGGTGGGT-3’; 5’-Thiol-GAGGACCCACCCACCCACCCTCCTCAAThiol-3’	DPV	Pb^{2+}	0.374	1 – 40	2 mM $K_4[Fe(CN)_6]$, $K_3[Fe(CN)_6]$ 0.1 M KCl	[54]
Au NPs-polypyrrole	5’-GGGTGGGTGGGTGGGT-3’; 5’-CCACCCACCC–$(CH_2)_6$–SH-3’	DPV	Pb^{2+}	2.9	2.4 – 120	PBS pH 7.4	[35]
Au NPs-polypyrrole	5-GGGTGGGTGGGTGGGT-3	DPV	Pb^{2+}	0.36	0.5 – 10	5 mM $K_4[Fe(CN)_6]$, $K_3[Fe(CN)_6]$, PBS pH 5.8	[55]
Au NPs@GO	5’-HS-TTTTTT CGATAACTCACTATrAGGAAGAGATG-3’;	Amperometry	Pb^{2+}	1.67×10^{-3}	5×10^{-3} – 1000	PBS pH 7.4	[31]

	5'-HS-TTTTTTCATCTCTTCTCCGAGCCGGTCGAAATAGTGAGT-3'						
Au NPs	HS-CACCCTCCCAC- 3'; HS-GGGTGGGTGGGTGGGTGGGT- 5'	Potentiometry	Pb^{2+}	8.5×10^{-3}	0.01 – 1000	0.1 M PBS pH 7.4	[22]
Au NPs and QD	Not reported	ECL	Pb^{2+}	0.24	0.1 – 10000	0.1 M PBS, 0.02 M $K_2S_2O_8$ pH 7.4	[27]
Au NPs and CNNF	Not reported	ECL	Pb^{2+}	4×10^{-5}	1 – 1000	0.1 M PBS, 0.1 M $K_2S_2O_8$, 0.1 M KCl pH 7.4	[30]
Au NPs	5′-SH-$(CH_2)_6$-TTCTTTCTTCGCGTTGTTTGTT-MB-3′	SWV	Hg^{2+}	0.62×10^{-6}	1×10^{-6} – 1	6-mercapto-hexanol, 20 mM Tris-HCl buffer	[34]

						pH 7	
Au NPs	5′-SH-AAAAAAAAAAAAAAAACGCGCG-3′; 5′-TTTTTTTTTTTTTTT-3′; 5′-SH-CGCGCGCGCGCG-3′	EIS	Hg^{2+}	0.05	0 – 200	0.1 M PBS pH 7	[56]
Au NPs	5'-HS-GCGCGCGCCCTTTTTCCCCCCCCCGCGCGCGC biotin-3'; 5'-FAM-GCGCGCGCCCTTTTTCCCCCCCCCGCGCGCGC-Dabcyl-3'; 5'-TTTTGGGCGAACACACAC-3'; 5'-SH-TTTTTTTTTTGGATTTTTTTTGACGATTTTTTT-MB-3'	DPV	Hg^{2+}	0.21×10^{-3}	0.35×10^{-3} – 3.5	10 mM PBS pH 7	[21]

rGO/ Au nanorods	5’-SHTTTTTT T-3’; 5’-biotin-TTT TTT T-3’	DPV	Hg^{2+}	0.24	1 – 200	-	[57]
Fe_3O_4@Au NPs	5’-SH-AAAATCACCCATGAGGCATCTTTAGCG-3’; 5’- Fc-TCATCCGTGAT-3’; 5’- MB-CGCTTTAGATG-3’	SWV	Hg^{2+}	1.7	10 – 100	20 mM Tris-HCl, 140 mM NaCl, 5 mM $MgCl_2$ pH 7.4	[3]
Ag@Au core shell	5’-CCC CCC CCC CCC TTC TTT CTT CCC CTT GTT TGT T-3’	SWV	Hg^{2+}	6×10^{-3}	0.01 – 0.16	0.05 M PBS pH 6	[24]
Au@Ag core shell	5’-SH-(CH2)6-AAA ATT TTG CTT TGG TTT-3’; 5’-SH-$(CH_2)_6$-AAA AAT TTC CTT TGC TTT-3’; 5’-SH-(CH2)6-GGG TAG GGC GGG TTG GGT-3’	SWV	Hg^{2+}	2.99×10^{-3}	9.97×10^{-3} – 99.7	PBS buffer pH 6.5	[1]

Au/MoS_2-MWCNT	5’-SH-C6-CGGCTTTTGTTTT-3’	DPV	Hg^{2+}	0.05	0.1 – 1000	Tris buffer pH 7.4	[58]
Au@HS-rGO	5′-SH-(CH2)6-TTGCTCTCTCGTT	DPV	Hg^{2+}	0.38	1 – 200	PBS pH 7.4	[59]
Au NPs and QD	Not reported	ECL	Hg^{2+}	4.1×10^{-3}	$0.01 – 0.1 \times 10^{-3}$	0.1 M PBS, 0.02 M $K_2S_2O_8$ pH 7.4	[27]
Fe_3O_4@SiO_2/ dendrimers/QD + Au	5’-TTCTTTGTTCCCCTTCTTTGTT-NH2-3’; 5’-AACAAAGAACCCCCCCCCC-(CH2)3-SH-3’	ECL	Hg^{2+}	2×10^{-9}	$20 \times 10^{-9} – 2000$	0.1 M PBS pH 7.4	[25]
Au NPs and QD	5’-CCA ACC ACA CCA ACC(CH2)6-NH2-3’; 5’-GGT TGG TGT GGT TGG TTC TTT CTT CCC TTG TTTGTT(CH2)6-SH-3’; 5’-SH-(CH2)6CAT ATC C-3’	ECL	Hg^{2+}	0.3×10^{-3}	$1 \times 10^{-3} –10000$	0.1 M PBS, 5 mM H_2O_2 pH 8	[28]

Au NPs	5’-TTCG TGTT GTGT TTCC AAA GGAT TCTC TACT CGTA-3’	ECL	Hg^{2+}	2×10^{-3}	0 – 0.2	150 mM PBS 1 μM $Ru(bpy)_3^{2+}$ 50 mM TPA pH 7.4	[29]
Au NPs	5’-SH-(-CH2)6-TTGCTCTCTCGTT-(-CH2)6-NH2-3’; 5’-TTCGTGTGTGCTT-3’	ECL	Hg^{2+}	0.2×10^{-4}	1×10^{-3} – 100	0.1 M PBS pH 7	[26]
Au@Ag-MoS_2 nanohybrid and QD	Calf thymus DNA	PEC	Hg^{2+}	5×10^{-3}	0.01- 100	0.1 M PBS 0.2 M Ascorbic acid pH 7.4	[60]
3D-rGO-Au	5’-GGTAATACGACTCACTATAGGGAGA TACCAGCTTATTCAAT	EIS	As^{3+}	1.9×10^{-6}	5.07×10^{-6} – 4×10^{-4}	PBS pH 7.4	[33]

	TTTACAGAACAACCAACGTCGCTCC GGGTACTTCTTCATCGAGATAGT AAGTGCAATCT-3’						
Carbon Au binanoparticles	5’-HS- GGTAATACGACTCACTATAGGG AGATACCAGCTTATTCAATTTTACA GAACAACCAACGTCGCTCCGGGT ACTTCTTCATCGAGATAGTAAGTGC AATCT-3’	SWV	As^{3+}	1.22	6.7 – 1334	0.1 mM $[Ru(NH_3)_6]^{3+}$, 10 mM PBS	[61]
Au NPs– CB	5’HS$(CH_2)_6$GGACTGTTGTGGTATTAT TTTTGG TTGTGCAGTATG3’	SWV	Cd^{2+}	1.2	8.9 – 400	10 mM PBS pH 7.45	[62]
Au NPs/CS	5’-HS-$(CH_2)_6$- ACCGACCGTGCTGGACTCTGGACTG TTGTGGTATTA	DPV	Cd^{2+}	0.04995×10^{-3}	0.001 – 100	PBS pH 7.4	[63]

	TTTTTGGTTGTGCAGTATGAGCGAG CGTTGCG-3’						
Fe_3O_4@Au NPs	5’-SH-AAAATCACCCATGAGGCATCTTTAG CG-3’; 5’- Fc-TCATCCGTGAT-3’; 5’- MB-CGCTTTAGATG-3’	SWV	Ag^+	3.4	0 – 400	20 mM Tris-HCl, 140 mM NaCl, 5 mM $MgCl_2$ pH 7.4	[3]

CNNF: carbon nitride nanofibers, GO: graphene oxide, QD: quantum dots, rGO: reduced graphene oxide, BSA: bovine serum albumin, MoS_2: molybdenum disulfide, MWCNT: multiwalled carbon nanotubes, GSH: glutathione, HS: thiol, MB: methylene blue, CB: carbon black, CS: chitosan, PBS: phosphate buffer, TPA: tripropylamine.

Table 2 Non-electrochemical aptasensors using gold nanoparticles for the detection of heavy metals

Modification	Aptamer	Technique	Heavy metal	LOD (nM)	Linear range (nM)	Operational conditions	Ref
Au NPs	5'-SH-$(CH_2)_6$-TTTTTTACCCAGGGTGGGTGGGTGGGT-3'; 5'-SH-$(CH_2)_6$-TTTTTTACCCACCC-3'	QCM	Pb^{2+}	4	5 – 200	25mM HEPES, 0.1 M NaCl pH 7.4	[64]
Au@Fe_3O_4 NPs	5'-SH C6-CGGCTTTTGTTTT-3'	MRS	Hg^{2+}	2.7	10 – 100 100 – 5000	-	[65]
Au NPs	5'-GGTTGGTGTGGTGGTTGGT-GTTGG-3'	SERS	Pb^{2+}	-	various	0.27mM HCl pH 2.8	[47]
Au@Ag NPs	5′Cy3-TTC TTT GTT CCC CTT CTT TGT TCC CCC CCC CC-SH-3′; 5′Rox-AAC AAA GAA-3′	SERS	Hg^{2+}	0.4×10^{-3}	0.001 – 1	No influence	[49]

SiO_2@Au core/shell	5'-HS-(CH2)6-TTTTTTTTTTGGGGGGGGAAAAAAAA-3'	SERS	Hg^{2+}	10	10 – 10^6	-	[48]
Au NPs	5'-SH-(CH2)6-GATTCCGTGCATGACTCAG-3'; 5'-SH-(CH2)6-CTGTGTCTTGCTCGGTATC-3'	LSPR	Hg^{2+}	0.7	1 – 50	0.05 M Tris-HCl buffer pH 6.8	[66]
(+)Au NPs	5′-TTT TTT TTT T-3′; 5′-GGT TGG TGT GGT TGG-3′; 5′-CTC ACG TAA ACT CAC GTA AA-3′	Chemiluminescence	Hg^{2+}	0.016	0.62 – 120 120 – 1200	HAc–NaAc Buffer pH 4	[67]
Au NPs	13 different aptamers	Visual	Pb^{2+}	2.5	10 – 500 500 – 25000	HEPES buffer pH 7.4	[68]
Au NPs	5'-GGTTGGGCGGGATGGGTG-3'	Colorimetry	Pb^{2+}	2.4	24 – 9660	7 < pH <8	[69]

Au NPs	5'-TCGGGTGTGGGTG GGTGGTGGTGGTTGTGGTGGTGGTG G-3'; 5'-CACCC ACACC CGATT TTTTT TTTTT-SH-3'; 5'-CCACC ACCAC CACAA CCACC ACCAC CACA-3'; 5'-TCGGG TGTGG GTGTC GGGTG TGGGTG-3'	Colorimetry	Pb^{2+}	25	10 – 500	-	[70]
Au NPs	HS-$(CH_2)_6$-GGGTGGGTGGGTGG	Colorimetry	Pb^{2+}	0.58×10^3	-	pH 7	[71]
Fe_3O_4-Au NPs-graphene	5'-biotin-GGGTGGGTGGGTGGGT-3'; 3'-CCACCCTCCCAC-5'	Colorimetry	Pb^{2+}	3	4.8 – 1400	(3-(N-morpholino) propanesulfonic acid) buffer pH 7	[10]

Au NPs	5’-TTT TTT TT-3’; 5’-TTT TTT TTT TTT TTT-3’; 5’-AAA AAA AAA AAA AAA-3’; 5’-AAA AAA AAA ATT TTT TTT TTT TTT T-3’; 5’-AAA AAA AAA AAA AAA AAA AAA AAA A-3’; 5’-AAA AAA AAA AAA AAA AAA AA-3’; 5’-AAA AAA AAA AAA AAA AAA AAA AAA AAA A-3’; 5’-AAA AAA AAA AAA AAA AAA AAA ATT TTT TTT TTT TTT TAA AAA AAA AAA AAA AAA AAA AA-3’;	Colorimetry	Hg^{2+}		various	PBS pH 7.4	[72]

	5’-AAA AAA AAA AAA AAA AAA AAA AAA AAA AAA AAA AAA AAA AAA AAA AAA AAA AAA AA-3’						
Au NPs	5′SH$(CH_2)_6$TCAGTTTGGC3′; 5′SH$(CH_2)_6$GCCTTTCTGA3′	Colorimetry	Hg^{2+}	1.4×10^{-3}	0.005 – 25	-	[36]
Au NPs	HS-$(CH_2)_6$-GGGTGGGTGGGTGG	Colorimetry	Hg^{2+}	2.49×10^{3}	-	pH 7	[71]
Au NPs	5’- GGTCACGCTTTCTTCTTTCTTTC-3’ 5’- GAA AGC GTG ACA CAG-3’ 5’- GTT TGT TTG TTG TTA GCG TGA CGG TC-3’ 5’- SH-TTT CAC GCT TTC-3’	Colorimetry	Hg^{2+}	0.9	1 – 10000	NEBuffer	[73]
Au NPs	5’-TCA TGT TTG TTT GTT GGC CCCCCT TCT TTC TTA-3’;	Colorimetry	Hg^{2+}	15	50 – 300	(3-(N-morpholino) propanesulfo	[74]

	5’-TTT GTT TGT TGG CCC CCC TTC TTT CTT A-3’					nic acid) buffer	
cationic AuNPs	5’-TTT TTT TTT T-3’; 5’-CCT CCC TCC TTT TCCACCCACC-3’; 5’-CCA ACCACA C -3’	Colorimetry	Hg^{2+}	0.049	0.82 – 62	HAc–NaAc buffer pH 4	[52]
Au NPs	5’-TCGAGATAGTAAGTGCAATCT-3’	Colorimetry	As^{3+}	2.4	13 – 400 400 – 1335	pH 8.5	[41]
CTAB-AuNPs	5’-GGTAATACGCTCACTATAGGGAGAT ACCAGCTTATTCAATTTTACAGAAC AAC CAACGTCGCTCCGGGTACTTCTTCAT CGAGATAGTAAGTGCAATCT-3’	Colorimetry	As^{3+}	225	0 – 1335	-	[39]

AuNPs	5'GGTAATACGACTCACTATAGGGAG ATACCAGCTTATTCAATTTTACAGA ACAACCAACGTCGCTCCGGGTACTT CTTCATCGAGATAGTAAGTGCAATC T-3'	Colorimetry	As^{3+}	2100	1000 – 10000	(3-(N-morpholino) propanesulfonic acid) buffer pH 7.3	[38]
Au NPs	5'-TTTTTTTTTT-3'	Colorimetry	Cd^{2+}	8.9×10^{-3}	8.9×10^{-3} – 3.5	Tris-HCl buffer pH 7.4	[37]
Au NPs	5'-ACCGACCGTGCTGGACTCTGGACTG TTGTGG. TATTATTTTTGGTTGTGCAGTATGAG CGAGCGTTGCG-3'	Colorimetry	Cd^{2+}	9.9	17.8 – 178	-	[75]
Au-MoS_2	5′-biotin-ACC GAC	Colorimetry	Cd^{2+}	6.2	8.9 – 4448	pH 7	[76]

	CGT GCT GGA CTC TGG ACT GTT GTG GTA TTA TTT TTG GTT GTG CAG TAT GAG CGA GCG TTG CG-3'; 5′–SH–CGC AAC GCT CGC TCA TAC TGC ACA ACC AAA -3'						
Au NPs	5'-CCCC CCCCCCCCCCCCCCCCCCCCCCCC -3'	Colorimetry	Ag^{+}	0.77	1 – 500	-	[20]
UCNPs-MNPs-GNPs	5'-Biotin-CGATCA CTA ACTATr AGG AAG AGATG-HS-3'; 5'-NH2-TGA GTG ATA AAG CTG GCC GAG CCT CTTCTC TAC-3'	Fluorometry	Pb^{2+}	5.7	25 – 1400	-	[23]
Au NPs and QD	5'-/3ThioMC3-D/CGATAACTCACTATrAGGAAGAGA TG-3';	Fluorometry	Pb^{2+}	16.7	50 – 4000	-	[43]

	5'- /5AmMC6/CATCTCTTCTCCGAGCCGG TCGA-AATAGTGAGT-3'						
AuNP and UCNP	5'-AAGGGT GGGT GGGT-3'; 5'-AAAAA AAAAA AAAAA AAAAA TTTTT CACCC TCCC AC -3'	Fluorometry	Pb^{2+}	4.1	0 – 50	20mM Tris-HCl buffer solution pH 7.4	[44]
Au NPs	5′ - b i o t i n - AAAAAAAAAATTCTTTCTTCCCCTT GTTTGTT-3′; 5′-biotin-AAAAAAAAAACACA AACAAGGCCAACA-3′	Fluorometry	Hg^{2+}	0.65	0.65 – 214.4	0.05 M Tris-HCl, 1% TritonX-100, 0.15 M NaCl pH 8	[45]
Au NPs	5'NH2C6-CTA CAG TTT CAC CTT TTC CCC CGT TTT GGT GTT T-3'; 5′ SH C6-GAA ACT GTA G-3'	Fluorometry	Hg^{2+}	60	200 – 20000	-	[46]

QCM: quartz crystal microbalance, MRS: magnetic relaxation switching, SERS: surface enhanced Raman spectroscopy, SiO_2: silica, CTAB: cethyltrimetylammonium bromide, LSPR: localized surface plasma resonance, UCNP: upconversion nanoparticles, MNP: magnetic nanoparticles, GNP: gold nanoparticles, HEPES: 4-(2-hydroxyethyl) piperazine ethanesulfonic acid sodium salt

Table 3 Aptasensors using metal oxide nanoparticles for the detection of heavy metals

Modification	Aptamer	Technique	Heavy metal	LOD (nM)	Linear range (nM)	Operational conditions	Ref
Ti- modified Co_3O_4	5'-GGACTGTTGTGGTATTAT TTTTGGTTGTGCAGTCC-3'	CV	Cd^{2+}	4.36×10^{-3}	1.8×10^{-3} – 0.13	0.1 M HAc-NaAc, 1.0 mM thionine pH 5.5	[11]
Cu_xO	5′- CAACGGTGGGTGTGGTTGG - 3'	EIS	Pb^{2+}	6.8	0.1 - 100	10 mM PBS, 0.1 M KCl, 5 mM $[Fe(CN)_6]^{3-/4-}$ pH 7.4	[77]
CdS-TiO_2, gold nanochains	5'-SH-GGGTGGGTGGGTGGGT-3'; 5'-ACCCACCCACCCACCC-3'	PEC	Pb^{2+}	1.6×10^{-3}	5×10^{-3} – 10	PBS pH 7	[78]

CeO_2	5'-MB-AAAAA-3'	DPV	As^{5+}	20.5	50 – 2000	10 mM HEPES, 200 mM NaCl pH 7.6	[79]
$Au@Fe_3O_4$ NPs	5'-SH C_6-CGGCTTTTGTTTT-3'	MRS	Hg^{2+}	2.7	10 – 100 100 – 5000	-	[65]
Graphene/Fe_3O_4-Au NPs	5'-biotin-GGGTGGGTGGGTGGGT-3'; 3'-CCACCCTCCCAC-5'	colorimetry	Pb^{2+}	0.24	4.8 - 1400	(3-(N-morpholino)propanesulfonic acid) buffer pH 7	[10]
Streptavidin-coated Fe_3O_4	5'-Biotin-AAAAAAAAAACATGTTAGTCGTTGCT-3'; 5'-NH_2-AGC TTC GTC TAT CTTG-3'	fluorescence	Hg^{2+}	1	1 – 1000	NaCl 137 mM, KCl 2.7 mM, Na_2HPO_4 10 mM, KH_2PO_4 2 mM pH 7.2	[2]
Magnetic beads	5'- Biotin - TTCTTTCTTCTTTC -3'; 5'- GTTTGTTGTTTGTT -3'; 5'- FAM – GAAAGAAGAAAGAA -3'	fluorescence	Hg^{2+}	0.2	2 - 160	137 mM NaCl, 2.7 mM KCl, 10 mM Na_2HPO_4, 2 mM KH_2PO_4	[80]
$Fe_3O_4@SiO_2$/	5'-TTC TTT GTT CCC CTT CTT TGTT-NH_2-3'	ECL	Hg^{2+}	2×10^{-9}	2×10^{-8}	0.1 M PBS pH 7.4	[25]

dendrimers/QD Au NPs					– 2000		
Fe_3O_4@Au NPs	5'-SH-AAAATCACCCATGAGGCATCTTTAGCG-3'; 5'- Fc-TCATCCGTGAT-3'; 5'- MB-CGCTTTAGATG-3'	SWV	Hg^{2+}	1.7	10 – 100	20 mM Tris-HCl, 140 mM NaCl, 5 mM $MgCl_2$ pH 7.4	[3]
Fe_3O_4@Au NPs	5'-SH-AAAATCACCCATGAGGCATCTTTAGCG-3'; 5'- Fc-TCATCCGTGAT-3'; 5'- MB-CGCTTTAGATG-3'	SWV	Ag^{+}	3.4	0 – 400	20 mM Tris-HCl, 140 mM NaCl, 5 mM $MgCl_2$ pH 7.4	[3]
Pt nanotubes Thionine labelled Fe_3O_4 /rGO NPs	5'-SH-(CH2)6-ACCGTGTTTGCCTTTGACCTC-3' 5'-GCTGTCGGATGAGGTCTTTGGCTTTCACGGT-3' 5'-CTCATCCGACAGC-(CH2)6-NH2-3'	DPV	Hg^{2+}	0.03	0.1 – 100	5 mM $K_3[Fe(CN)_6]$/ $K_4[Fe(CN)_6]$, 0.1 M KCl, 10 mM PBS	[81]
Fe_3O_4 / graphene	5′-H_2N-$(CH_2)_6$-TTTTTACCCA GGGTGGGTGGG TGGGT-3′	ICP-MS	Pb^{2+}	0.24	1.45 – 4100	pH 7	[82]

Ag-coated magnetic core shell NPs	5’-GGT TGG TGT GGT TGG-3’	AAS	Pb^{2+}	48	159 – 4831	pH 7	[83]

CdS cadmium sulfide; PEC photoelectrochemical; MB methylene blue; MRS magnetic relaxation switching; rGO reduced graphene oxide; ICP-MS inductively coupled plasma mass spectrometry; AAS atomic absorption spectrometry